Redox Biology 80 (2025) 103527

Contents lists available at ScienceDirect

Redox Biology

journal homepage: www.elsevier.com/locate/redox

FNDC5/irisin mitigates the cardiotoxic impacts of cancer chemotherapeutics by modulating ROS-dependent and -independent mechanisms

Manish Kumar [a,b], Abhishek Singh Sengar [a], Anushree Lye [a,h], Pranesh Kumar [c], Sukhes Mukherjee [d], Dinesh Kumar [a], Priyadip Das [e], Suvro Chatterjee [f], Adele Stewart [g], Biswanath Maity [a,h,*]

[a] Centre of Biomedical Research, Raebareli Road, Lucknow, Uttar Pradesh, 226014, India
[b] Academy of Scientific and Innovative Research (AcSIR), Ghaziabad-201002, India
[c] Institute of Pharmaceutical Science, University of Lucknow, Uttar Pradesh, 226007, India
[d] Department of Biochemistry, AIIMS Bhopal, Saketnagar, Bhopal, Madhya Pradesh, India
[e] Department of Chemistry, SRM Institute of Science and Technology, Tamil Nadu, 603203, India
[f] Department of Biotechnology, Burdwan University, West Bengal, 713104, India
[g] Department of Neuroscience & Pharmacology, University of Iowa, Iowa City, IA, 52242, USA
[h] Department of Biological Sciences, Bose Institute, EN 80, Sector V, Kolkata, West Bengal, 700091, India

A B S T R A C T

Cardiotoxicity remains a major limiting factor in the clinical implementation of anthracycline chemotherapy. Though the etiology of doxorubicin-dependent heart damage has yet to be fully elucidated, the ability of doxorubicin to damage DNA and trigger oxidative stress have been heavily implicated in the pathogenesis of chemotherapy-associated cardiomyopathy. Here, we demonstrate that fibronectin type III domain-containing protein 5 (FNDC5), the precursor protein for myokine irisin, is depleted in the hearts of human cancer patients or mice exposed to chemotherapeutics. In cardiomyocytes, restoration of FNDC5 expression was sufficient to mitigate reactive oxygen species (ROS) accumulation and apoptosis following doxorubicin exposure, effects dependent on the irisin encoding domain of FNDC5 as well as signaling via the putative irisin integrin receptor. Intriguingly, we identified two parallel signaling cascades impacted by FNDC5 in cardiomyocytes: the ROS-driven intrinsic mitochondrial apoptosis pathway and the ROS-independent Ataxia Telangiectasia and Rad3-Related Protein (ATR)/Checkpoint Kinase 1 (Chk1) pathway. In fact, FNDC5 forms a co-precipitable complex with Chk1 alluding to possible intracellular actions for this canonically membrane-associated protein. Whereas FNDC5 overexpression in murine heart was cardioprotective, introduction of FNDC5-targeted shRNA into the myocardium was sufficient to trigger Bax up-regulation, ATR/Chk1 activation, oxidative stress, cardiac fibrosis, loss of ventricular function, and compromised animal survival. The detrimental impact of FNDC5 depletion on heart function could be mitigated via treatment with a Chk1 inhibitor identifying Chk1 hyperactivity as a causative factor in cardiac disease. Though our data point to the potential clinical utility of FNDC5/irisin-targeted agents in the treatment of chemotherapy-induced cardiotoxicity, we also found significant down regulation in FNDC5 expression in the hearts of aged mice that attenuated the cardioprotective impacts of FNDC5 overexpression following doxorubicin exposure. Together our data underscore the importance of FNDC5/irisin in maintenance of cardiac health over the lifespan.

1. Introduction

Anthracyclines (doxorubicin, daunorubicin, idarubicin, and epirubicin), which remain amongst the most used cancer chemotherapeutics due to their efficacy in the treatment of solid tumors and hematological malignancies, can trigger life-threatening and dose-limiting cardiac toxicity. In a large meta-analysis, 17.9 % of doxorubicin-treated patients were found to have developed sub-clinical cardiac dysfunction with 6.3 % presenting with heart failure [1]. Adverse cardiac complications resulting from anthracycline exposure are particularly problematic for childhood cancer survivors [2], an ever growing population, whose risk for congestive heart failure is increased by 2.4 fold or 5.2 fold with cumulative anthracycline doses of <250 mg/m^2 or >250 mg/m^2, respectively [3]. Thus, there is considerable interest in delineating the molecular mechanisms driving anthracycline cardiotoxicity and identifying novel means to protect the heart from damage during and after chemotherapy.

The ability of doxorubicin to kill cancer cells involves recruitment of two intersecting pro-apoptotic pathways: activation of the DNA damage signaling cascade [4] and production of reactive oxygen species (ROS)

* Department of Biological Sciences Bose Institute Unified Academic Campus EN 80, Sector V, Kolkata, 700091, WB, India.bmaity@jcbose.ac.in
E-mail address: bmaity28@gmail.com (B. Maity).

https://doi.org/10.1016/j.redox.2025.103527
Received 11 November 2024; Received in revised form 17 December 2024; Accepted 1 February 2025
Available online 4 February 2025

[5–10]. Cardiomyocytes are particularly sensitive to oxidant damage from anthracyclines due to their high metabolic demand and mitochondrial volume as compared to glycolytic cells [11]. However, doxorubicin doses required to trigger oxidative myocyte damage *in vitro* [11] are several fold higher than levels achieved in human cancer patients [12], emphasizing the potential importance of repeated drug exposure and accumulation of cellular damage over time. Indeed, at lower doses, doxorubicin does not kill cardiomyocytes, but instead triggers a senescence-like state characterized by oxidative stress, mitochondrial dysfunction, Ca^{2+} dyshomeostasis, and disrupted electrical conduction [13]. Importantly, increased cellular senescence has been observed in the hearts of doxorubicin-treated cancer patients [14], and, in mice, elimination of therapy-induced senescent cells improves cardiac function following doxorubicin treatment [15]. Several senescence-related pathways are activated by doxorubicin including the DNA repair proteins Ataxia Telangiectasia and Rad3-Related Protein (ATR) and Checkpoint Kinase 1 (Chk1), which are recruited to the site of single stranded DNA breaks [16]. ATR phosphorylates Chk1 on two conserved serine residues (317 and 345) driving enhanced Chk1 activity critical for initiation of DNA repair [17,18]. Indeed, preventing ATR activation is cardioprotective in doxorubicin-treated mice [19]. However, given the importance of the DNA damage signaling response in cancer killing actions of doxorubicin, direct modulation of ATR/Chk1 activity might also compromise doxorubicin's therapeutic efficacy.

In the search for factors capable of preventing heart failure, there is increasing interest in the cardioprotective impacts of the exercise-induced chemokine irisin. Irisin is generated from proteolytic cleavage of the fibronectin type III domain-containing protein 5 (FNDC5) gene product by proteases of the disintegrin and metalloproteinase (ADAM) family [20]. FNDC5 cleavage separates the irisin-containing fibronectin-type III domain from the extracellular signal peptide responsible for membrane targeting and protease recruitment, and the hydrophobic transmembrane and carboxy-terminus [21]. Irisin production is highest in cardiac muscle and depletion of plasma irisin has linked to cardiovascular diseases [22–24]. Irisin administration also improves cardiac function in several rodent heart failure models [25–27]. Further, knockout of FNDC5 exacerbated cardiac fibrosis and loss of ventricular function in mice following chronic doxorubicin administration [28] whereas cardiac FNDC5 overexpression is cardioprotective [29]. Several irisin targets have been implicated in the cardioprotective actions of FNDC5 though most studies have heavily focused on mechanisms driving acute myocyte loss as opposed to the potential long-term impacts of FNDC5/irisin on myocyte functional integrity. Intriguingly, FNDC5 also regulates cardiogenesis and expression of FNDC5 is increased in fully differentiated cardiomyocytes [30–32]. Notably, cardiac-specific FNDC5 overexpression or irisin infusion attenuates aging-related cardiac dysfunction and prevents myocyte senescence *in vitro* [33].

Here, we delineate a novel signaling mechanism for FNDC5 in the myocardium whereby the FNDC5 protein interacts directly with Chk1 and prevents Chk1-driven myocyte death following doxorubicin exposure and in the aging myocardium. Intriguingly, though FNDC5 does limit doxorubicin-driven oxidative stress in the heart, the FNDC5-Chk1 pathway is ROS-independent. Our data suggest that maintenance of FNDC5 expression is essential for long-term cardiac health and resilience to cardiotoxic insult.

2. Materials and methods

2.1. Reagents

A full list of reagents can be found in Table S1.

2.2. Mice

Male Swiss albino mice (25–30 g) were raised on a balanced laboratory diet and given tap water and food *ad libitum* throughout the study as per NIN, Hyderabad, India. Mouse housing facilities were held at 20 ± 2 °C, 65 %–70 % humidity, on a 12/12-h day/night cycle. Animals were maintained according to International Animal Ethics Committee Guidelines. Unless otherwise noted, experiments have been performed using animals between 2 and 4 months of age. Experimental mice were euthanized by inhalation anesthesia followed by cervical dislocation and disposed of following CPCSEA guidelines. All experiment were performed by a user blinded to experimental group.

2.3. Drug treatment regimens

For the chronic chemotherapy treatment, mice were given multiple doses of doxorubicin (cumulative dose of 45 mg/kg i.p.; 9 mg/kg every other week), 5-FU (cumulative dose of 200 mg/kg i.p.; 40 mg/kg every other week), or cisplatin (cumulative dose of 40 mg/kg i.p.; 8 mg/kg every other week) for a total of 10 weeks. 9 weeks after the final drug dose, mice were euthanized, and multiple tissues/blood were collected for the downstream analysis.

2.4. Cloning and construct generation

The full-length FNDC5 coding sequence was PCR-amplified from human blood cDNA using our previously published protocol [34]. FNDC5 deletion constructs were generated using overlapping primer-based PCR amplification, and subsequently cloned into the pEGFP-N1 vector. Information about the primers used for constructing all the constructs are provided Table S2. To generate viral constructs for *in vivo* overexpression of FNDC5, we first isolated the full length of FNDC5 sequence from mouse brain tissue and cloned it into the PMD20 vector, as described above. Subsequently, the lentiviral vector for mFNDC5 was generated via subcloning into the pLenti CMV Puro DEST cloning vector (Addgene, Watertown, MA, USA) and this lentiviral vector was then packaged using the pMD2.G VSV-G envelope-expressing plasmid (Addgene) and psPAX2 (Addgene). Lentiviral particles were generated in AC-16 cells following a standard protocol.

2.5. Intracardiac gene delivery

To overexpress FNDC5 in heart, a construct encoding mouse FNDC5 or vector-only control was introduced to the murine heart via intracardiac injection when mice were either young (2 months old) or aged (24 months old). A total of 70 μL of lentivirus, which contained 2×10^8 particles of either mFNDC5-Lenti or an empty control vector virus, were prepared for delivery with Invivofectamine 3.0 (Thermo Fisher Scientific, Waltham, MA, USA) and administered directly into the heart. 8–10 weeks after viral injection, the chronic doxorubicin treatment protocol was initiated as described above. Mice were euthanized 10 weeks after the final drug dose and tissues were collected for downstream analyses.

To deplete FNDC5 in heart, 1 week old wild type mice received 5×10^8 lentiviral vector particles containing scramble or FNDC5-targeted small hairpin RNA (shRNA) (Santacruz Biotechnology, Paso Robles, CA, USA) in a 40 μl volume via intra-cardiac injection as previously described [35]. ShRNA particles were packaged for delivery with Invivofectamine 3.0 (Thermo Fisher Scientific). Immunoblotting was performed on heart tissue extracted from adult experimental mice to assess the efficiency of *in vivo* delivered shRNA. Following shRNA administration, body weight (1X/week), food intake (1–2X/week), and survival were monitored. A separate cohort of animals received injections of the Chk1 inhibitor LY2606368 (cumulative dose of 250 mg/kg i.p.; 50 mg/kg every other week) or saline beginning 15 days after viral injection for 10 weeks. A final group of mice were administered doxorubicin according to the chronic protocol outlined above. The treatment continued for 10 weeks after which mice were euthanized and samples collected for downstream analyses.

2.6. Histology and immunohistochemistry (IHC)

Paraffin-embedded formalin-fixed mouse and human heart tissue sections were stained with Masson trichome (Sigma, St. Louis, MO) to detect collagen deposition indicative of cardiac fibrosis. Regents were used following the manufacturer's protocols. Immunohistochemical staining of both mouse and human tissue sections was carried out as per a standard protocol [35]. For IHC and Masson Staining in murine experimental cohorts, 7-10 sections were stained from the heart of each animal with 5 pictures randomly selected from each slide. For IHC and Masson staining in human patient samples, 7-10 sections were stained from each heart with 5 pictures randomly selected from each slide. The blue-stained collagen in tissue section image stained with Masson trichrome was processed using the "Threshold" tool of ImageJ software (NIH, USA) and the fraction of the total area that was stained blue was quantified. Quantification of immunostaining was also performed using built-in tools in the Image J software package.

2.7. Cardiovascular Phenotyping

We employed two-dimensional echocardiography to determine cardiac function. Using an ultrasound system (Vivid S5 system, GE Healthcare, USA) in M-mode, we measured the left ventricular parameters and ejection fraction on lightly sedated mice, both before and after drug treatments or the introduction of FNDC5 shRNA into the heart via intracardiac injection.

2.8. Immunoblotting

Tissues were swiftly isolated from mice and flash-frozen in liquid nitrogen. Tissue homogenates and cell lysates were prepared in RIPA buffer containing protease and phosphatase inhibitors (Abcam, Cambridge, UK), quantified, and probed as previously described [36]. Twenty μg of protein per sample was subjected to SDS-PAGE and immunoblotting using standard techniques. Immunoblots were developed using the chemiluminescence method with secondary antibodies labeled with HRP. Antibody dilution and catalog information can be found in Table S3. Densitometric quantification of western blots was performed utilizing Image J software (NIH). Protein expression was normalized to loading control (β-Actin) and expressed relative to control conditions.

2.9. Isolation and culture of murine ventricular cardiomyocytes (VCM) and fibroblasts (VCF)

Primary ventricular cardiomyocytes (VCM) and fibroblasts (VCF) were isolated from 8 to 10-week-old adult mice according to a published protocol [37]. Cells were transduced with lentiviral vectors encoding shFNDC5 or control shRNA (Santacruz Biotechnology) according to the manufacturer's instructions.

2.10. Cell culture

The AC-16 human cardiomyocyte cell line & H9C2 rat cardiomyocyte cell line (Merck, Darmstadt, Germany) was maintained in DMEM supplemented with 10 % FBS (Gibco, Waltham, MA, USA) within a 37 °C incubator with 5 % CO_2. Information on cell lines can be found in Table S4.

2.11. Drug treatment of cultured cells

For FNDC5 overexpression in cultured AC-16 cells or murine VCM and VCF, lentiviral FNDC5 was introduced into cells using Invivofectamine 3.0 (Thermo Fisher Scientific) according to the manufacturer's protocol. A group of cells were transduced with an empty vector as a control. Cells were pre-treated with the integrin αVβ5 inhibitor cilengitide (10 μM, 24 h), the Chk1 inhibitor LY2603618 (10 μM, 24 h), or the glutathione donor and ROS scavenger N-acetyl cysteine (NAC; 5 mM, 12 h) followed by treatment with doxorubicin (3 μM, 16 h). To attenuate FNDC5 expression in cells, cells were transfected with FNDC5-targeted shRNA (Santacruz Biotechnology, Paso Robles, CA, USA) or a scramble control. Cells were pre-treated as above with NAC, the Chk1 inhibitor, or irisin (200 ng/ml, 24 h) followed by doxorubicin treatment (3 μM, 16 h).

2.12. Immunoprecipitation

Lysates were prepared from AC-16 cells (3×10^6), and the protein concentration was measured using the BCA protein assay (Thermo Fisher Scientific). 200 μg of protein was incubated in IP lysis buffer (50 mM Tris, 5 mM EDTA, 250 mM NaCl and 0.1 % Triton X-100) and bait antibodies (GFP, FNDC5, or control mouse IgG) for 12 h on a rotor at 4 °C. 30 μl of Protein G sepharose beads (Abcam) were pre-cleared, equilibrated and then added to lysate. After a 2-h incubation, bead slurries were centrifuged and washed 3X with IP buffer. The Immunocomplex were eluted using non-reducing Laemmli buffer at 95 °C and were then subjected to SDS-PAGE and immunoblotting with the corresponding prey antibody (FNDC5 or Chk1).

2.13. ELISAs and enzymatic assays

A summary of commercially available kits used for the quantification of superoxide dismutase (SOD), glutathione peroxidase (GPX), cell death (apoptosis; cytoplasmic histone-associated DNA fragments), mitochondrial Ca^{2+}, mitochondrial membrane potential ($\Delta\psi_M$), and irisin is available in Table S5. Cells, tissues, or samples were collected and processed in according to the instructions provided by the manufacturer.

2.14. Measurement of ROS generation

ROS generation was estimated in both tissues and primary cells using the cell-permeable oxidation-sensitive probe, CM-H_2DCFDA as described previously [38]. In summary, the cells were harvested via centrifugation, subjected to triple wash with ice-cold PBS, re-suspended in PBS and incubated with 5 μM CM-H_2DCFDA (Sigma) for 20 min at 37 °C. After incubation cells were again washed and lysed in PBS with 1 % Tween 20. The determination of ROS levels was performed by the ratio of dichlorofluorescein excitation at 480 nm to emission at 530 nm. The CM-H_2DCFDA assay is utilized as a general oxidative stress indicator and not as a detector of a specific oxidant due to known limitations of the probe [39].

2.15. Cell senescence model

To induce senescence of AC-16 & H9C2 cells, cells were starved at 0.1 % FBS DMEM medium overnight to achieve synchronization, and then doxorubicin (0.1 μM, 24 h) was added into the cell culture medium. Cells were maintained in culture for a further 5 days with media changed daily to maintain doxorubicin concentration.

2.16. YASARA homology modelling of FNDC5 & in-silico molecular docking and molecular dynamics (MD) simulations

For generating protein-protein interaction model between human CHK1 and FNDC5, the alpha-fold 3D structures available on Uniprot database for human Isoform 1 of CHK1 (Alpha fold ID: AF-O14757-F1 |) and human FNDC5 protein (Alpha fold ID: AF-Q8NAU1) were used. First, the binding modes of CHK1 in complex with FNDC5 were generated using ZDOCK webserver application (https://zdock.umassmed.edu) [40,41]. The molecular complex between CHK1-FNDC5 with highest binding energy was further evaluated for solution stability under biological conditions by performing a 359.25 ns molecular dynamics

(MD) simulation in explicit water solvent using YASARA Dynamics software (version 21.8.27.W.64 employing the AMBER14 force field) [42].

The MD simulation was performed as per the details and parameters described previously [43,44]. The MD simulation was performed with CHK1 molecule as receptor molecule (Met1-Thr476; excluded segment Asp262-Arg376; named as Chain A) and the FNDC5 fragment as the ligand (residues Met76-Ile179; named as Chain B). The MD snapshots were saved after every 250 ps and total 1438 MD trajectories were generated during the MD simulations which were analyzed using YASARA macro "md_analysis.mcr". The various energy terms were calculated using AMBER14 forcefield parameters [45,46]. The MD simulation and trajectory analysis was performed on HP Z Series Workstation (64 GB of RAM, 24 Core Intel Processor and 64-bit Windows 10 operating system). The trajectories generated after MD simulation experiments were used to estimate the root mean square deviations (RMSD) and radius of gyration (Rg), chain-wise root mean square fluctuations (RMSF), solvent accessible surface area (SASA), and hydrogen bonding between protein and solvent. For the analysis of amino acid residues present on protein-protein interaction interface, the solvent accessible surface area (SASA) calculations were performed using the InterProSurf Webserver (http://curie.utmb.edu/usercomplex.html) [47]. The residues showing a significant change in the SASA value were considered most likely to be on the interaction interface (Table S6).

2.17. In silico pathway analysis

To determine the pathway enrichment of FNDC5 the pathway analysis was performed *in silico* using the Enrichr (https://maayanlab.cloud/Enrichr/enrich) tool. The pathways predicted to be

impacted by FNDC5 in heart with their p-values are provided in Table S8.

2.18. Histological characterization of chemotherapy patient samples

To categorize patient samples according to their cardiac health status, tissues from chemotherapy patients were stained with Masson Trichome (as above) to detect fibrotic remodeling. In collaboration with a pathologist, sections were evaluated and assigned. "Control" samples were obtained from individuals with no history of cancer or chemotherapy treatment as well as no known cardiac issues. An effort was made to ensure that controls contained an equal male/female ratio (~50 %) and age range (50–80) as samples isolated for the "chemotherapy-exposed" group. Detailed information about the cause of death and any co-morbid conditions for all individuals is provided in Table S7.

2.19. Additional statistical analysis information

A Student's t-test was employed to compare groups in datasets comprising only two groups (1A, 2A, 8B, 8C). Nominal p-values are reported for these datasets, and no adjustments were applied.

For the remaining datasets with more than two groups, either a one-way ANOVA (1 variable; 2B, 3C-D, 4A, 4E, 5A, S4) or a two-way ANOVA (2 variables; 1B, 1C, 2C, 3A-B, 4B-D, 4F–H, 5B–C, 6C, 7A-E, 8A, 8D, S1, S2A-C, S3A-E, S5A-E, S7A-B) was utilized, and post-hoc adjustments were performed using the Sidak method to account for multiple comparisons. Adjusted p-values are reported for datasets analyzed in this manner. Kaplan Meier curves were generated to visualize mouse survival over time following FNDC5 depletion in heart and statistical comparisons performed (7F). A standard linear regression was generated to assess the correlation between FNDC5 expression in heart and patient age (8E).

2.20. Study approval

We have performed the mouse experiments at the Aryakul College of Pharmacy & Research, Lucknow and AIIMS Bhopal. Animals were obtained post clearances from the Animal Ethics Committee (1896/PO/Re/S/16/CPCSEA/2022/3 - Aryakul College of Pharmacy & Research and AIIMS/BPL/IAEC/2024/051 - AIIMS Bhopal were handled following International Animal Ethics Committee Guidelines and in agreement with the Guide for the Use and Care of Laboratory Animals (NIH). We have used post-mortem human tissue samples and collected it from the Department of Forensic Medicine, Sagore Dutta Medical College &Hospital, Kolkata, West Bengal post obtaining the ethical clearance from CBMR Ethics Committee (IEC/CBMR/Corr/2018/14/2). Detailed patient information for samples utilized in this work has been provided in the supplementary.

3. Results

FNDC5 is downregulated in cancer patients exposed to anthracyclines and associated with activation of the ATR/Chk1 DNA damage signaling cascade – FNDC5 expression is high in cardiac muscle and an *in silico* analysis of signaling cascades predicted to be impacted by FNDC5 include those critical for heart function (e.g., adrenergic signaling, cardiac muscle contraction, GAP junction formation, and calcium signaling) and/or implicated in cardiovascular disease (e.g., dilated cardiomyopathy and hypertrophic cardiomyopathy) (Table S8). Though circulating irisin levels have been measured in individuals with heart failure [22–24], cardiac expression of the irisin precursor FNDC5 has not be assayed in cancer patients with chemotherapy-induced cardiomyopathy. We obtained post-mortem heart tissue samples from individuals with a history of chemotherapy who died of heart failure (chemotherapy) or controls with no history of adverse cardiac events and confirmed elevations in cardiac fibrosis (Fig. 1A) and markers of hypertrophy and heart failure such as β myosin heavy chain (β-MHC) and atrial natriuretic peptide (ANP) in hearts from the chemotherapy exposed group (Fig. 1C). Significant depletion in FNDC5 expression as measured via either immunohistochemistry (Fig. 1B) or immunoblot (Fig. 1C) was also evident in the chemotherapy-exposed myocardium. We also noted robust induction of the ATR/Chk1 DNA damage cascade including the DNA damage marker γH2AX, ATR, Chk1 phosphorylation on the ATR target site (S345), and Chk1-target p73 (Fig. 1B and C) as well as the pro-apoptotic Bcl-2 family member Bax, a major mediator of mitochondrial-dependent apoptosis.

FNDC5 overexpression in heart prevents doxorubicin-induced activation of the ATR/Chk1 pathway – To investigate a possible causative role for FNDC5 depletion in induction of ATR/Chk1 in the chemotherapy exposed myocardium, we first tested if doxorubicin treatment led to FNDC5 down-regulation in murine heart, confirming a significant reduction in FNDC5 immunoreactivity following treatment with doxorubicin (Fig. 2A), 5-flurouracil (Fig. S1A), or cisplatin (Fig. S1B). To manipulate FNDC5 expression in heart we utilized intracardiac injection of adenoviral vectors encoding FNDC5 shRNA (FNDC5 KD) or a construct encoding full-length FNDC5 (FNDC5 OE). Importantly, decreasing or increasing FNDC5 expression had a corresponding impact on circulating levels of irisin peptide (Fig. 2B) validating our approach. Supraphysiological FNDC5 expression also mitigated doxorubicin-induced activation of the ATR/Chk1 signaling cascade and decreased expression of ANP, but not β-MHC in heart tissue (Fig. 2C). Notably, cardiac FNDC5 overexpression alone was sufficient to decrease cardiac ATR expression, Chk1 phosphorylation and p73 levels (Fig. 2C).

Tuning FNDC5 expression modulates cardiomyocyte sensitivity to doxorubicin-dependent cytotoxicity – Next, we overexpressed or knocked down FNDC5 expression in cultured human (AC-16 cells) or primary murine ventricular cardiomyocytes (VCM). It is important to note that, whereas overexpression of FNDC5 did decrease Chk1 phosphorylation in AC-16 cells, VCM, or ventricular cardiac fibroblasts it also led to induction of ANP, Troponin T, and β-MHC after 48 h (Fig. S2), all of which are markers of heart failure and indicators of cardiomyocyte dysfunction. Thus, cardiomyocyte viability likely requires maintenance of

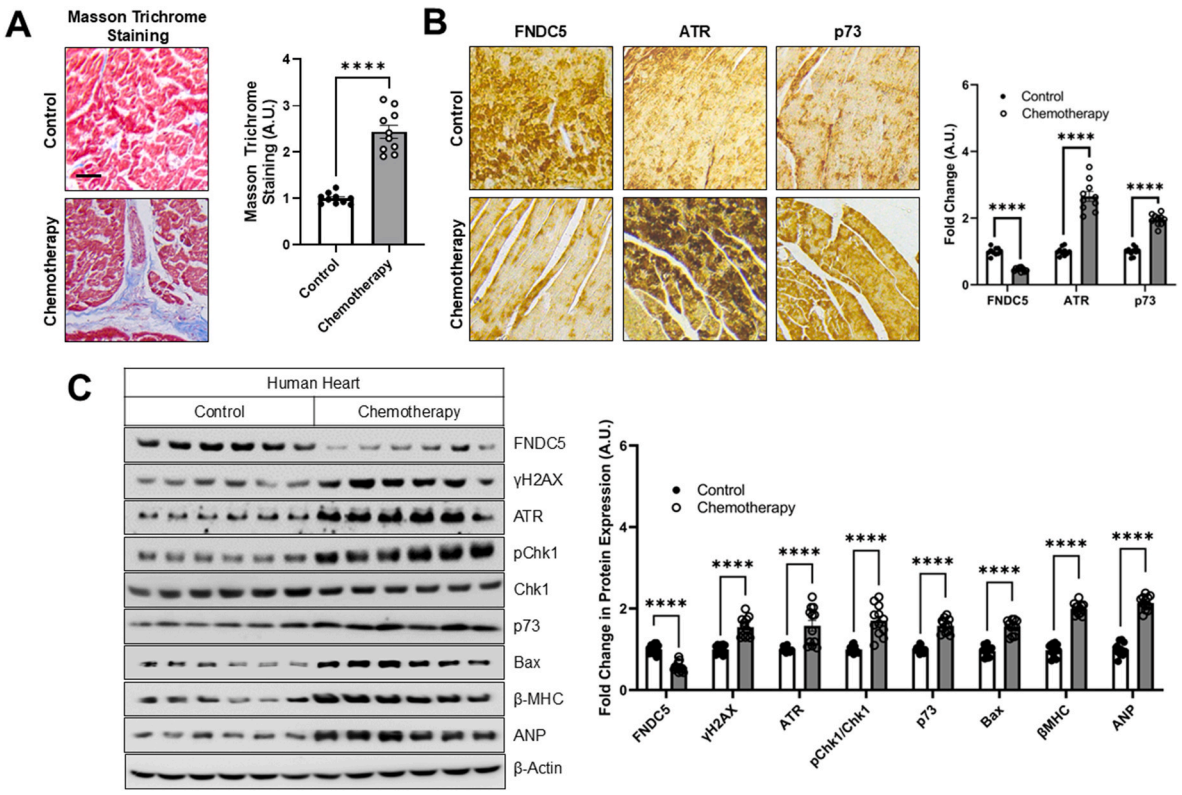

Fig. 1. – FNDC5 is depleted in the hearts of human cancer patients following chemotherapy exposure. (A) Representative Masson Trichrome staining and quantification in control (n = 10) and patients with a history of chemotherapy (n = 10) [scale bar = 100 μm]. (B) Representative immunostaining and quantification of cardiac FNDC5, ATR, and p73 in control (n = 10) and patients with a history of chemotherapy (n = 10) [scale bar = 100 μm]. (C) Representative immunoblots and quantification of cardiac FNDC5, γH2Ax, ATR, pChk1, p73, Bax, β-MHC, and ANP expression in controls and patients with a history of (n = 12/group). A detailed information regarding history of chemotherapy patients and controls is provided in Table S1 β-Actin serves as a loading control for immunoblots. The data were analyzed by student's t-test or two-way ANOVA with Sidak's post-hoc test. ****$P < 0.0001$. The data are presented as mean ± SEM.

FNDC5 levels within a prescribed range. To prevent significant FNDC5-dependent cellular stress, we confined experiments investigating the impact of FNDC5 on doxorubicin-dependent myocyte damage to earlier time points. After 16 h, FNDC5 overexpression in AC-16 cells resulted in a small, but significant decrease in doxorubicin-dependent Chk1 phosphorylation, expression of p73 and Bax and induction of ANP and β-MHC (Fig. S3A). Importantly, preventing FNDC5 depletion resulted in a 50 % reduction in death of AC-16 cells following doxorubicin treatment (Fig. S3B). Conversely, FNDC5 knockdown (KD) was sufficient to increase expression of phospho-Chk1, p73, Bax, β-MHC, and ANP (Fig. S3C) and increase oxidative stress (Fig. S3D) and apoptosis (Fig. S3E) in AC-16 cells. In addition, FNDC5 depletion sensitized cells to doxorubicin treatment as evidenced by increased pChk1, p73, Bax, and ANP levels as well as ROS and apoptosis in doxorubicin treated FNDC5 KD cells as compared to control cells with intact FNDC5 expression (Figs. S3C–E).

The ability of FDNC5 to prevent ATR/Chk1 activation and cell death requires irisin – To test if the ability of FNDC5 to ameliorate the cardiotoxic actions of doxorubicin involved irisin signaling, we treated FNDC5 knockdown AC-16 cells with recombinant irisin and confirmed that induction of phospho-Chk1, p73, Bax, β-MHC, and ANP (Fig. 3A) as well as the increase in apoptosis (Fig. 3B) resulting from FNDC5 depletion were reduced following irisin supplementation. Next, we exposed AC-16 cells to doxorubicin following expression of FNDC5 or a vector control and in the presence or absence of the irisin integrin αVβ5 receptor inhibitor cilengitide [48]. These experiments confirmed that FNDC5 overexpression prevented doxorubicin-dependent up-regulation of phospho-Chk1, p73, Bax, β-MHC, and ANP (Fig. 3C) and apoptosis (Fig. 3D), but the impact of FNDC5 overexpression was lost in the presence of cilengitide. Together, these data suggest that the ability of FNDC5 to modulate Chk1 activity requires irisin release and signaling via its cell surface receptor. Deletion of the irisin-encoding segment of FNDC5 also partially blocked the ability of FNDC5 to prevent doxorubicin-dependent release of pro-inflammatory cytokines tumor necrosis factor α (TNFα) and interleukin 6 (IL-6) (Fig. S4). Together, these data demonstrate that the ability of FNDC5 to protect cardiomyocytes from doxorubicin-dependent damage requires release and autocrine signaling of irisin.

FNDC5 blocks ATR/Chk1 activation via a ROS-independent mechanism – Given prior evidence linking FNDC5 to suppression of doxorubicin-dependent oxidative stress [29], we hypothesized that the ability of FNDC5 to prevent ATR/Chk1 activation may also involve antioxidant action in cardiomyocytes. Indeed, we found that bidirectional modulation of FNDC5 expression in AC-16 cells resulted in corresponding changes in levels of antioxidants GPX and SOD (Fig. 4A). In addition, whereas FNDC5 depletion sensitized cells to doxorubicin-dependent induction of GPX and SOD (Fig. 4B), FNDC5 overexpression also partially suppressed oxidative stress following doxorubicin exposure (Fig. 4C). Irisin supplementation was sufficient to mitigate GPX and SOD activation and ROS generation following FNDC5 depletion (Fig. 4D) and inhibition of irisin signaling with cilengitide prevented the beneficial impact of FNDC5 overexpression on GPX, SOD, and ROS in doxorubicin-treated cardiomyocytes (Fig. 4E). Thus, the antioxidant effects of FNDC5 require irisin release and signaling.

Chk1 phosphorylation is activated by mitochondrial-derived oxidant generation, and, in turn, impacts translation of the mitochondrial genome [49]. In seeking to identify a potential mechanism linking FNDC5 signaling to ROS generation in myocytes, we hypothesized that FNDC5 might influence mitochondrial function, a key source of intracellular H_2O_2 production that drives Chk1 phosphorylation [49].

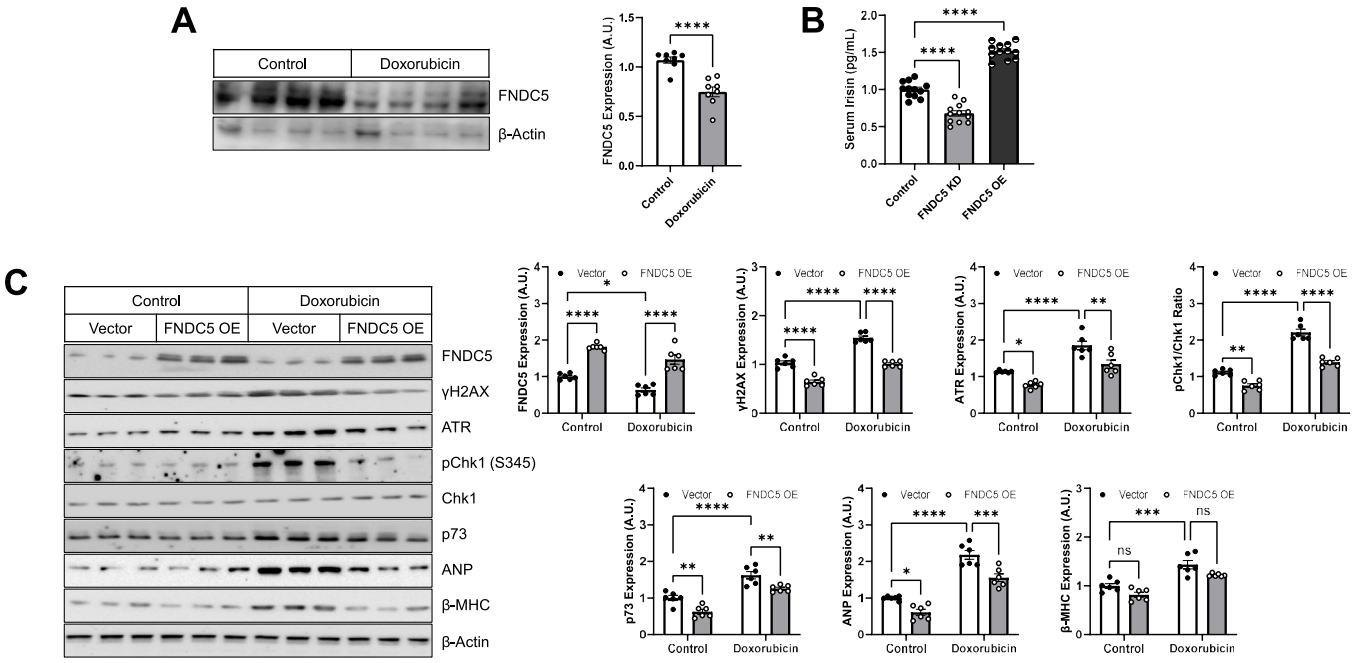

Fig. 2. – FNDC5 overexpression in heart attenuates Doxorubicin-dependent ATR/Chk1 activation. (A) Representative immunoblot and quantification of FNDC5 expression in hearts isolated from Doxorubicin (9 mg/kg, i.p. biweekly; cumulative dose of 45 mg/kg) or saline treated mice (n = 8). (B) Irisin levels quantified in serum isolated from mice that received an intracardiac injection of FNDC5-targeted shRNA or a viral vector encoding FNDC5 (n = 12). (C) After the intracardiac injection of an FNDC5 encoding viral construct or vector control into mouse myocardium, mice (n = 6) received either Doxorubicin (9 mg/kg, i.p. biweekly; a cumulative dose of 45 mg/kg) or saline starting at 9 weeks of age. Samples for analyses were collected one week after the final Doxorubicin dose. Representative immunoblots and quantification of FNDC5, γH2Ax, ATR, pChk1, p73, ANP, and β-MHC expression. β-Actin serves as a loading control for immunoblots. Data were analyzed by student's t-test or one- or two-way ANOVA with Sidak's post-hoc test. *$P < 0.05$, **$P < 0.01$, ***$P < 0.001$, ****$P < 0.0001$. ns = not significant. Data are presented as mean ± SEM.

Indeed, viral FNDC5 overexpression in AC-16 cells was sufficient to increase expression in both mitochondrial (e.g., complex 1 protein NADH dehydrogenase subunit 1, ND1) or nuclear (e.g., complex II protein cytochrome *b*-*c*1 complex subunit 2, UQCRC2) encoded mitochondrial electron transport chain proteins (Fig. 4F). Moreover, whereas doxorubicin altered mitochondrial Ca^{2+} flux (Fig. 4G) and triggered loss of mitochondrial membrane potential ($\Delta\psi_M$) (Fig. 4H), initial steps in the intrinsic apoptotic signaling cascade, the impact of doxorubicin on mitochondrial function was mitigated following FNDC5 overexpression (Fig. 4G and H). Together these data demonstrate that FNDC5 plays a role in ensuring mitochondrial integrity and limiting oxidative stress.

As the ATR-Chk1 cascade can be activated in response to oxidative stress, effects that require Chk1 phosphorylation on S296 [50], we hypothesized that the ability of FNDC5 to influence Chk1 would be ROS-dependent. However, whereas the ROS scavenger N-acetyl cysteine (NAC) decreased doxorubicin-driven Chk1 phosphorylation at S296 16 h following drug addition, FNDC5 overexpression had no impact (Fig. 5A). Indeed, the ability of FNDC5 depletion to trigger up-regulation of pChk1 (S345), p73, and β-MHC was not affected by NAC, though we did note a decrease in Bax induction (Fig. 5B), ANP generation (Fig. 5B), and cell death (Fig. 5C) in FNDC5 knockdown cells following NAC pre-treatment. These data allude to the possibility that FNDC5 impacts two parallel pathways in myocytes: ROS/Bax/apoptosis and the ATR/Chk1/p73 pathway. In addition, whereas release of compensatory hypertrophic factors such as ANP appear dependent on oxidative stress, the maladaptive switch from production of α-to β-MHC, which impairs cardiomyocyte contractility [51,52], is ROS-independent. In further support of parallel mechanisms driving doxorubicin-driven cardiotoxicity, either NAC (Fig. S5B) or an inhibitor of Chk1 (LY2606368, Chk1i) (Fig. S5D) decrease doxorubicin-dependent myocyte apoptosis. However, the effect of NAC on Bax expression was greater as compared to the Chk1/p73 axis (Fig. S5A). Conversely, Chk1i did not impact Bax expression in doxorubicin treated cells (Fig. S5C) but did decrease doxorubicin-driven ROS generation (Fig. S5E).

FNDC5 binds to Chk1 – We next considered an alternate hypothesis involving a direct interaction between the uncleaved FDNC5 molecule and Chk1. First, we performed molecular docking experiments with human Chk1 (Met1-Lys261; Met377-Thr476) and FNDC5 (Met76-Ile179) (Figs. S6A and S6B). The Chk1-FNDC5 complex with the highest binding affinity is depicted in Fig. 6A. Residues exhibiting the most significant change in solvent accessible surface area (SASA) upon binding of FNDC5 and Chk1 are summarized in Table S6 and depicted for Chk1 (Y227, D235, M433, L456, I471) and FNDC5 (W93, W165, F172, Y176, I178) in red (Fig. 6A). Molecular dynamics (MD) simulations were performed to evaluate the stability of the Chk1-FNDC5 complex [53] (Figs. S6C–G) and confirmed that the secondary structure (Fig. S6D) and binding energy (Fig. S6E) of both proteins remained consistent throughout the simulation. Indeed, FNDC5 and Chk1 form a co-precipitable complex in AC-16 cells that could be disrupted via elimination of the irisin-encoding domain of FNDC5 (Fig. 6B), which includes W93, a residue identified in our molecular modeling experiments. Finally, whereas altering FNDC5 expression in cardiomyocytes failed to impact the subcellular localization of Chk1, FNDC5 depletion or overexpression led to increased or decreased levels of phosphorylated Chk1 specifically in the nucleus (Fig. 6C). These data demonstrate that, though FNDC5 and Chk1 form a complex in cells, the primary function of FNDC5 in in modulation phosphorylation and nuclear translocation.

FNDC5 depletion damages the heart via a Chk1-dependent mechanism – To test if FNDC5-dependent Chk1 regulation is cardioprotective, we evaluated the impact of Chk1 inhibition following FNDC5 depletion *in*

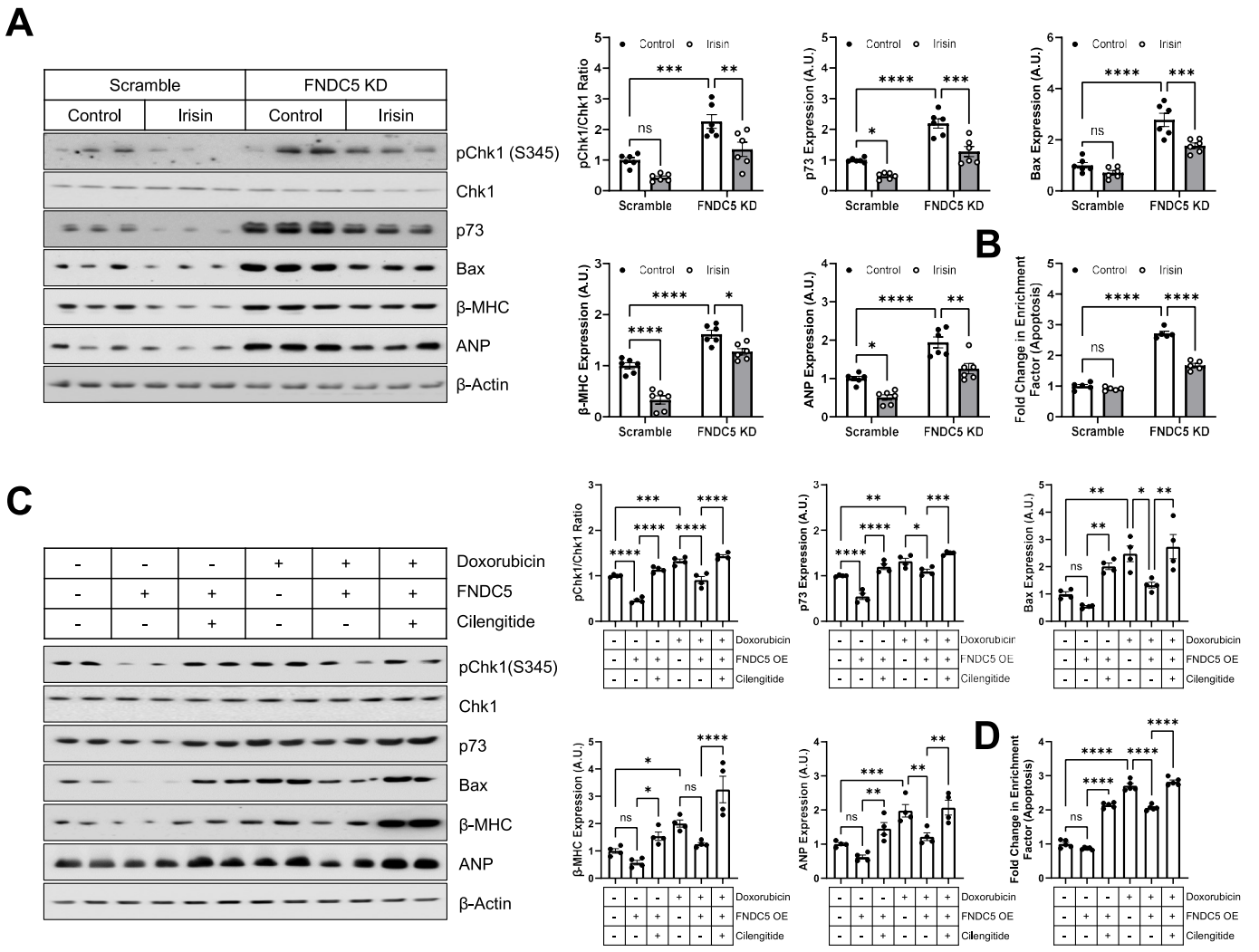

Fig. 3. – The ability of FNDC5 to suppress ATR/Chk1 activation requires irisin signaling. (A–C) AC-16 cells were pre-treated with irisin (200 ng, 24 h), and scramble or FNDC5-specific shRNA was inserted. (A) Representative immunoblots and quantification of pChk1, p73, Bax, β-MHC, and ANP (n = 6). (B) Apoptosis (cytoplasmic histone-associated DNA fragments; n = 5). (D–F) AC-16 cells were transduced with plasmids encoding FNDC5 (FNDC5 overexpression, OE) or vector control, pre-treated with Cilengitide (10 μM, 24 h), and then exposed to Doxorubicin (3 μM, 16 h). (C) Representative immunoblots and quantification of pChk1, p73, Bax, βMHC, and ANP (n = 6). (D) Apoptosis (cytoplasmic histone-associated DNA fragments; n = 5). β-Actin serves as a loading control for immunoblots. Data were analyzed by one- or two-way ANOVA with Sidak's post-hoc test. *$P < 0.05$, **$P < 0.01$, ***$P < 0.001$, ****$P < 0.0001$. ns = not significant. Data are presented as mean ± SEM.

vitro and *in vivo*. In AC-16 cells, treatment with a Chk1 inhibitor did decrease phospho-Chk1, p73, β-MHC, and ANP (Fig. S7A), but failed to impact Bax expression (Fig. S7A) and had only a small impact on cell death (Fig. S7B). Similar, though not identical results were obtained *in vivo* following introduction of FNDC5 shRNA into the hearts of young adult mice (2 months). Chk1i decreased phospho-Chk1, p73, β-MHC, and ANP as well as Bax expression resulting from FNDC5 depletion in the murine myocardium (Fig. 7A and B). Chk1 inhibition also ameliorated the deleterious impact of FNDC5 knockdown on cardiac fibrosis (Fig. 7C) and ventricular function (Fig. 7D). The impacts of Chk1 inhibition on cardiac oxidative stress induced by FNDC5 depletion were more modest with Chk1i treatment decreasing GPX and SOD activity but not CMH_2-DCFDA fluorescence (Fig. 7E). Importantly, cardiac FNDC5 knockdown also compromised the long-term survival of mice (Fig. 7F). Together, these data point to a role for FNDC5 in the prevention of cardiac damage via its ability to inhibit Chk1.

FNDC5 overexpression fails to prevent doxorubicin-dependent cardiotoxicity in aged mice As FNDC5 knockdown compromised murine longevity, we next tested the impact of FNDC5 overexpression on doxorubicin-induced cardiomyopathy in aged (24 months old) mice. We were surprised to observe that, unlike results obtained in younger animals, FNDC5 overexpression failed to suppress γH2AX, p73, ANP, or β-MHC up-regulation following exposure of aged mice to doxorubicin, though FNDC5 overexpression did decrease Chk1 phosphorylation (Fig. 8A). These results may be due to age dependent FNDC5 depletion in the heart (Fig. 8B), a phenomenon we also observed in higher passage, senescent cultured myocytes following serum starvation and low dose doxorubicin exposure (Fig. 8C). Indeed, whereas knockdown of FNDC5 in heart had no impact on total expression of ATR or Chk1 in young mice, FNDC5 depletion triggered robust γH2AX, ATR, and Chk1 induction in aged mice (Fig. 8D) indicating a remarkable sensitivity of aged mice to genomic instability resulting from loss of FNDC5. In support of a possible role for FNDC5 depletion in cardiac aging in humans we noted that, in both chemotherapy exposed patients and unexposed control subjects, FNDC5 expression significantly declines as a function of age (Fig. 8E). The outline of the story is presented as the schematic in Fig. 9.

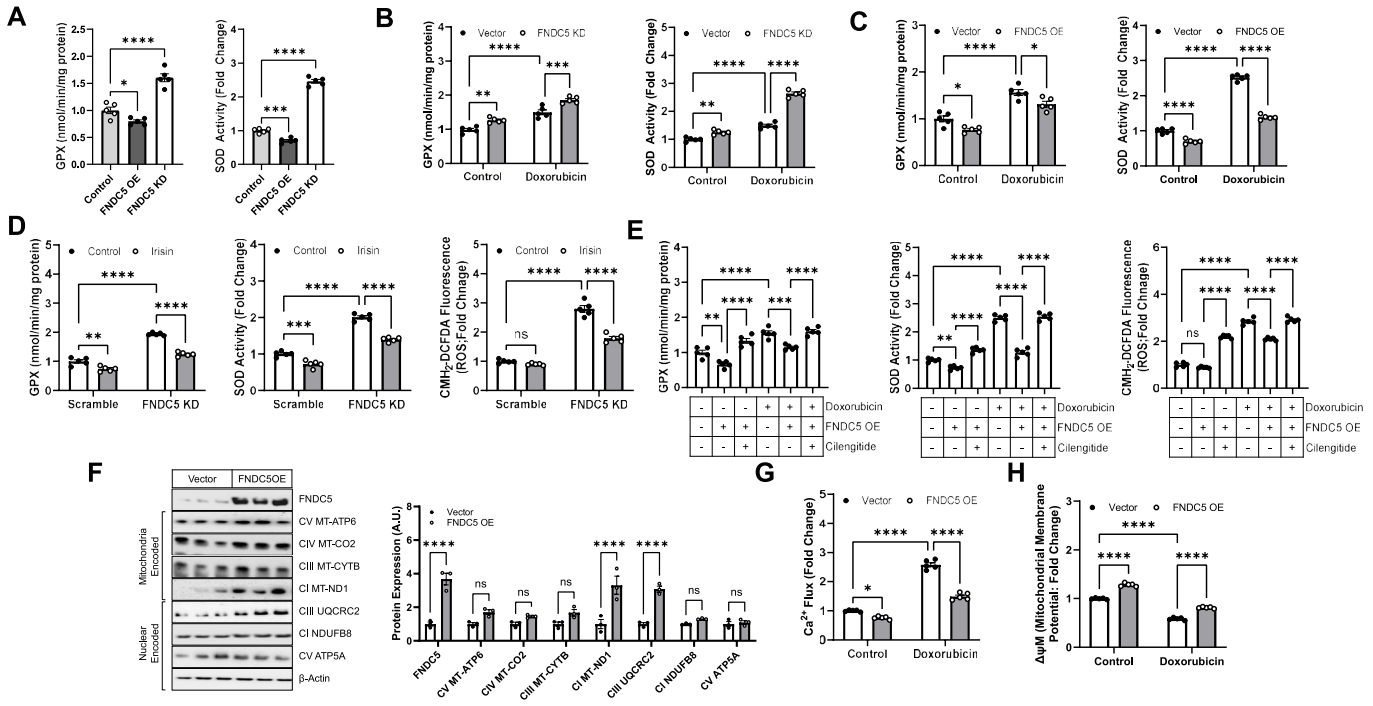

Fig. 4. – FNDC5 depletion increases oxidative stress and compromises mitochondrial function. AC-16 cells were transduced with either a plasmid encoding FNDC5 (FNDC5 overexpression, OE) or vector control or FNDC5-specific shRNA (FNDC5 KD) or scramble shRNA. (A) Baseline glutathione peroxidase (GPX) activity (n = 5) and superoxide dismutase (SOD) activity (n = 5). GPX and SOD activity (n = 5) in (B) FNDC5 KD or (C) FNDC5 OE cells treated with doxorubicin (3 μM, 16 h). (D) AC-16 cells expressing scramble or FNDC5-shRNA were pre-treated with irisin (200 ng, 24 h). GPX and SOD activity (n = 5) as well as CM-H_2-DCFDA fluorescence (ROS; n = 5) are shown. (E) AC-16 cells were transduced with plasmids encoding FNDC5 (FNDC5 overexpression, OE) or vector control, pre-treated with Cilengitide (10 μM, 24 h), and then exposed to Doxorubicin (3 μM, 16 h). GPX and SOD activity (n = 5) as well as CM-H_2-DCFDA fluorescence (ROS; n = 5) are shown. (F) AC-16 cells (n = 3) were transduced with a virus encoding FNDC5 (FNDC5 overexpression, OE) or vector control. Representative immunoblots and quantification of FNDC5, mitochondrial translated proteins (CV MT-ATP6, CIV MT-CO2, CIII MT-CYTB and CI MT-ND1) and nuclear translated proteins (CIII UQCRC2, CI NDUFB8 and CV ATP5A). (G–H) FNDC5 OE cells were treated with doxorubicin (3 μM, 16 h) and (G) mitochondrial Ca^{2+} (n = 5) and (H) mitochondrial membrane potential ($\Delta\psi_M$, n = 5). β-Actin serves as a loading control for immunoblots. Data were analyzed by one- or two-way ANOVA with Sidak's post-hoc test. *$P < 0.05$, **$P < 0.01$, ***$P < 0.001$, ****$P < 0.0001$. ns = not significant. Data are presented as mean ± SEM.

4. Discussion

Dose limiting cardiotoxicity remains a critical barrier to the clinical implementation of chemotherapeutic regimens containing doxorubicin. One pharmacological strategy employed to limit doxorubicin cardiotoxicity is the topoisomerase inhibitor dexrazoxane. However, whereas cardiac-specific topoisomerase-IIβ (TOP2B) deletion is cardioprotective following doxorubicin exposure in preclinical models [4] and dexrazoxane is approved for clinical use in the pediatric population [54,55], there is evidence that the drug induces genomic instability [56] that may be detrimental in cancer patients. Thus, alternative targets are sought that would allow for cardioprotection without impairing the therapeutic efficacy of chemotherapeutic agents or inducing more severe adverse events. Here, we identify FNDC5, downregulated in response to doxorubicin in humans or mice exposed to chemotherapy and in the aged murine myocardium, as a novel cardioprotective factor that prevents doxorubicin-dependent cardiac damage via two parallel mechanisms: suppression of the ATR/Chk1 DNA damage signaling cascade and alleviation of oxidative stress and mitochondria-dependent cell death. FNDC5 knockdown in heart was sufficient to trigger Chk1 phosphorylation on the ATR-targeted site S345 and increase expression of pro-apoptotic Bax. Conversely, FNDC5 overexpression in heart mitigated doxorubicin-dependent ATR induction, Chk1 phosphorylation, and p73 up-regulation. Intriguingly, FNDC5 forms a co-precipitable complex with Chk1 in cardiomyocytes, evidence alluding to direct modulation of Chk1 activity by either FNDC5 or irisin. Regardless, maintenance of FNDC5 expression and irisin production may represent a viable means to improve cardiac function in patients at high risk for chemotherapy-dependent cardiomyopathy.

The unique susceptibility of cardiomyocytes to doxorubicin-dependent cytotoxicity remains an area of ongoing speculation, but one hypothesis posits that their high metabolic demand and mitochondrial volume of sensitizes cardiomyocytes to oxidant damage [11]. Indeed, elimination of ROS-generating enzymes such as NADPH oxidases (NOXs) [10] improves whereas depletion of antioxidants such as SOD worsens doxorubicin-dependent heart damage [57]. Prior reports have demonstrated that irisin suppresses ROS production in vascular endothelial cells and neurons by targeting NOXs, inducible nitric oxide synthase (iNOS), and/or inflammatory signaling cascades [58–60]. Similarly, in cardiomyocytes, irisin treatment or FNDC5 overexpression reduces doxorubicin-dependent oxidative stress and apoptosis by improving mitochondrial dynamics, effects shown to require the transcription factor nuclear factor erythroid 2 p45-related factor 2 (Nrf2), a key regulator of cellular redox balance, or the kinase AKT [28,29]. Our data largely agree with these prior reports confirming that FNDC5 overexpression decreases oxidative stress triggered by doxorubicin whereas cardiac FNDC5 knockdown alone was sufficient to increase ROS and sensitize cardiomyocytes to doxorubicin-induced oxidative damage. Intriguingly, however, whereas antioxidant treatment did partially prevent Chk1 phosphorylation at S345 in doxorubicin exposed cardiomyocytes, it fails to decrease Chk1 activation following FNDC5 depletion. Similarly, Chk1 inhibition partially mitigates doxorubicin-dependent ROS generation, but has no effect on Bax up-regulation, an initiator of the mitochondrial apoptosis pathway. Thus, the pathway we have uncovered linking FNDC5/irisin to ATR/Chk1 signaling is distinct from the previously identified function of

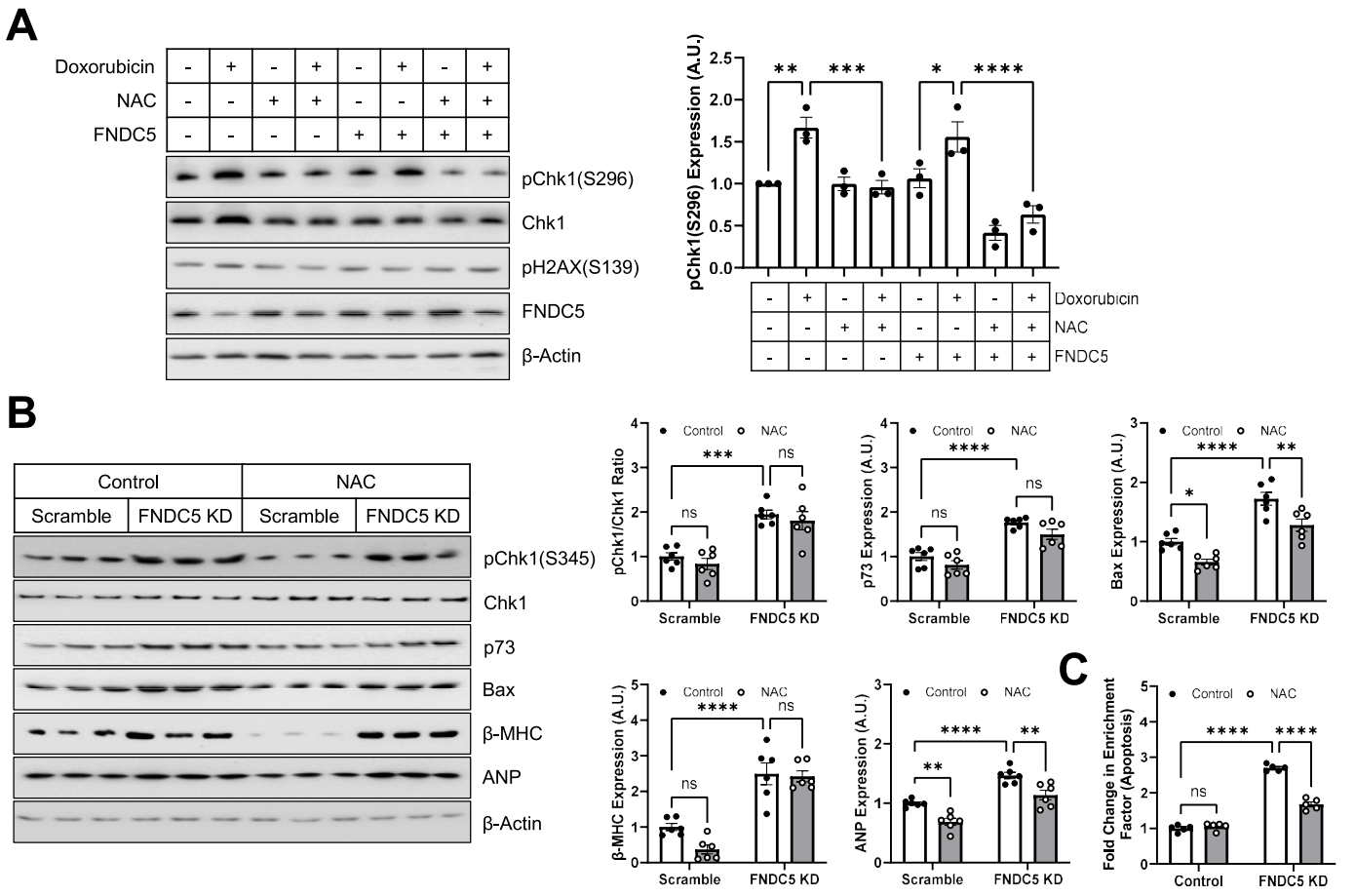

Fig. 5. – The ability of FNDC5 to decrease oxidative stress is not required for mitigation of Doxorubicin-dependent Chk1 activation. (A) AC-16 cells were transduced with plasmids encoding FNDC5 (FNDC5 overexpression, OE) or vector control, pre-treated with NAC (5 mM, 12 h), and then exposed to Doxorubicin (3 μM, 16 h). Representative immunoblots and quantification of pChk1(S296), pH2AX(S139), and FNDC5 are shown (n = 3). (D–E) AC-16 cells were transduced with vectors encoding scramble or lentiviral FNDC5-specific shRNA pre-treated with NAC (5 mM, 12 h). (B) Representative immunoblots and quantification of pChk1, p73, Bax, βMHC, and ANP (n = 6). (C) Apoptosis (cytoplasmic histone-associated DNA fragments; n = 5). β-Actin serves as a loading control for immunoblots. Data were analyzed by one- or two-way ANOVA with Sidak's post-hoc test. *$P < 0.05$, **$P < 0.01$, ***$P < 0.001$, ****$P < 0.0001$. ns = not significant. Data are presented as mean ± SEM.

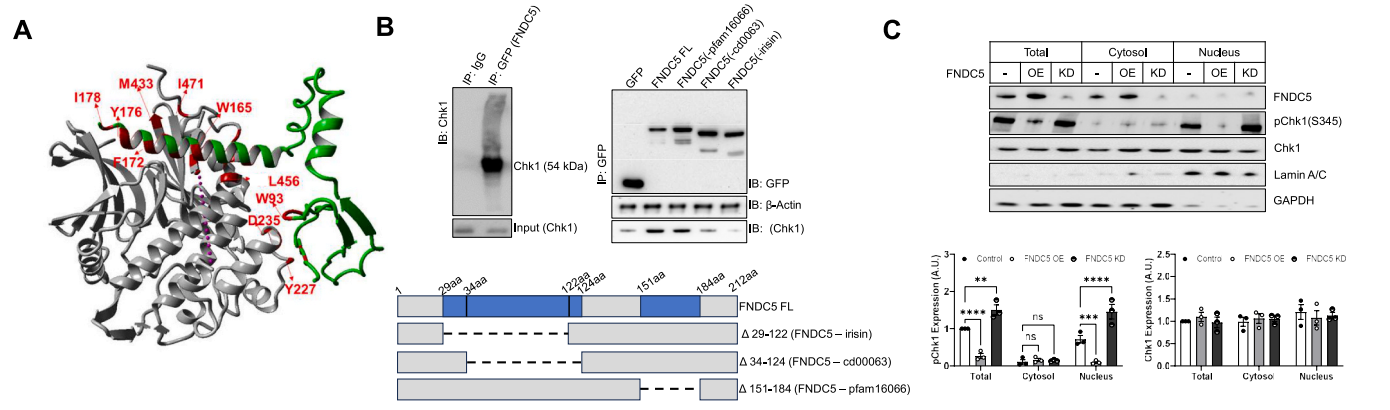

Fig. 6. – FNDC5 forms a complex with Chk1 in VCM. (A) *In silico* modeling of the FNDC5-CHK1 supports a direct interaction. The best docking pose for the FNDC5-CHK1 complex was predicted using a ZDOCK molecular docking experiment. Some of the residues present on the protein-protein interaction interface are highlighted in red text labels. (B) Co-immunoprecipitation (Co-IP) of FNDC5 with Chk1 from human AC-16 cardiomyocytes (left panel). Co-IP of Chk1 with FNDC5 deletion constructs transfected into human AC-16 cardiomyocytes (right panel). Constructs lacking the irisin (Δ29-122), fibronectin III domain (Δ34-124), or hydrophobic transmembrane domain (Δ151-184) were tested for Chk1 binding. (C) Expression of FNDC5, Chk1, phosphorylated Chk1, Lamin A/C, and GAPDH in total cell lysates or the cytosolic and nuclear fractions of AC-16 cells following either FNDC5 overexpression or knockdown (n = 3). Data were analyzed by one-way ANOVA with Sidak's post-hoc test. **$P < 0.01$, ***$P < 0.001$, ****$P < 0.0001$. ns = not significant. Data are presented as mean ± SEM.

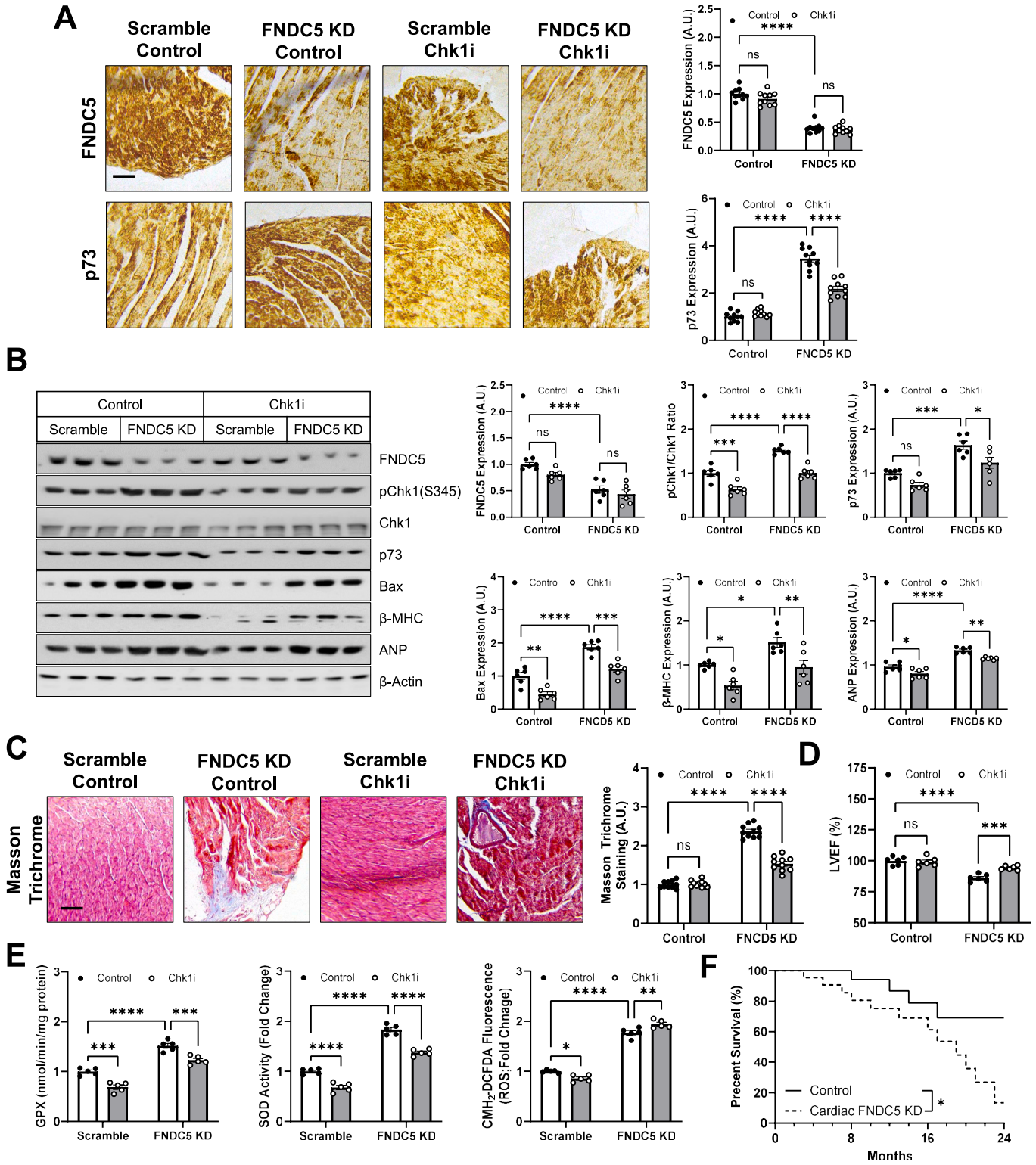

Fig. 7. – FNDC5 depletion triggers cardiac dysfunction by increasing Chk1 activity. Scramble or lentiviral FNDC5-targeted shRNA were introduced into the murine myocardium via intracardiac injection. Administration of scramble or lentiviral FNDC5-shRNA via intracardiac injection. Beginning at age 9 weeks, the Chk1 inhibitor LY2606368 (250 mg/kg cumulative dose; 50 mg/kg biweekly for 10 weeks) or saline. Samples were collected 1 week after the last dose later for biochemical and histological analyses. (A) Representative immunostaining and quantification of cardiac FNDC5 and p73 (n = 10) [scale bar = 100 μm]. (B) Representative immunoblots and quantification of FNDC5, pChk1, p73, Bax, βMHC, and ANP (n = 6). (C) Masson Trichrome staining in heart tissue sections (n = 10) [scale bar = 100 μm]. (D) Left ventricular ejection fraction (LVEF) (n = 6). (E) Oxidative stress measures including GPX/SOD activity (n = 5) and CM-H_2-DCFDA fluorescence (ROS; n = 5). (F) Survival curves of FNDC5-knockout and control wild-type mice. N = 18 in the wild-type group and N = 30 in the FNDC5-knockout group. β-Actin serves as a loading control for immunoblots. Data were analyzed by two-way ANOVA with Sidak's post-hoc test. *$P < 0.05$, **$P < 0.01$, ***$P < 0.001$, ****$P < 0.0001$. ns = not significant. Data are presented as mean ± SEM.

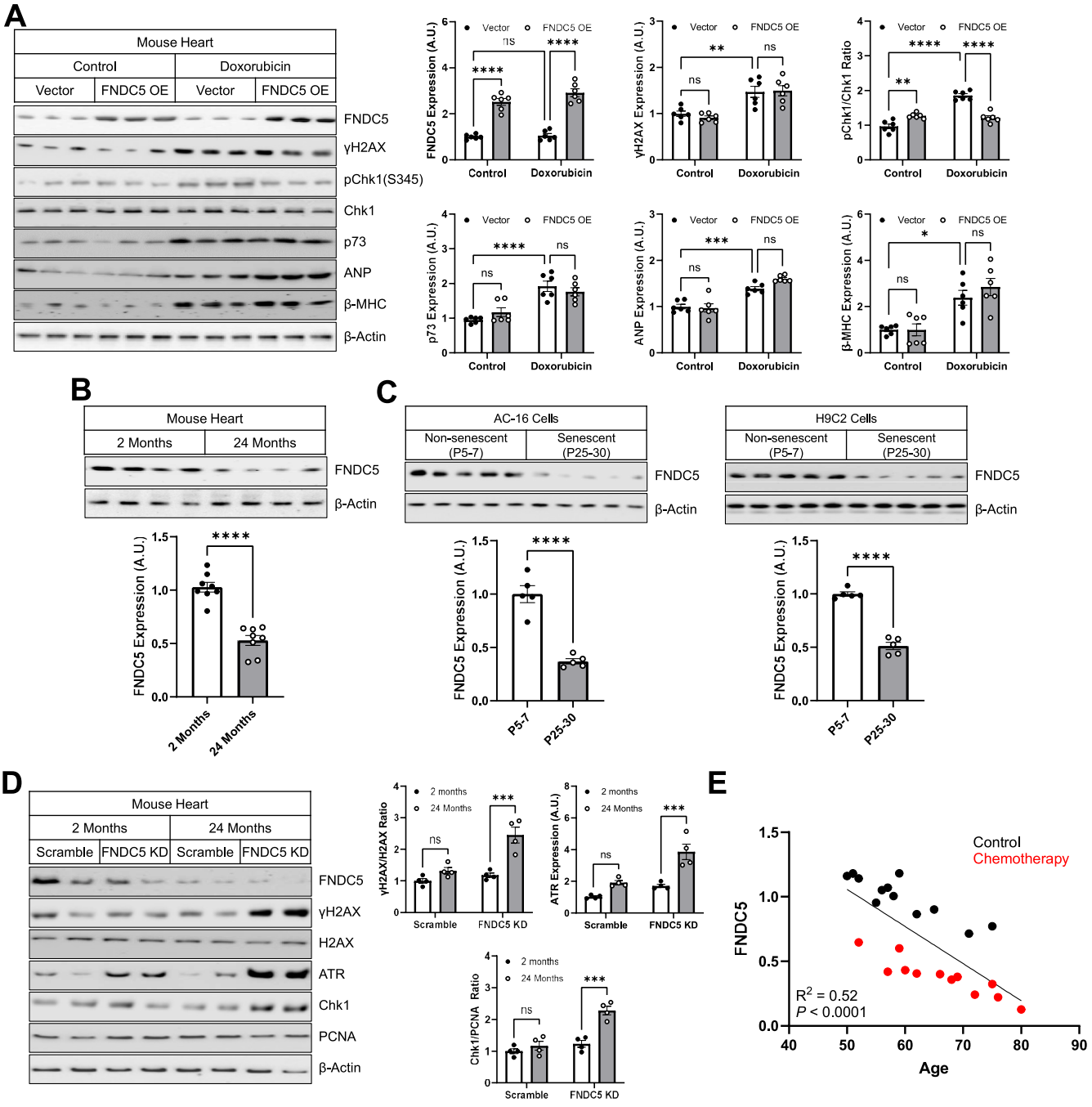

Fig. 8. – Cardiac FNDC5 is depleted with age resulting in increased susceptibility to cardiotoxic insult. (A) A lentiviral FNDC5 encoding viral construct or vector control was introduced into the mouse myocardium of one-month-old mice (n = 8). Beginning at age 2 months, mice received either Doxorubicin (9 mg/kg, i.p. biweekly; a cumulative dose of 45 mg/kg) or saline. Samples for analyses were collected one week after the final Doxorubicin dose. Representative immunoblots and quantification of FNDC5, γH2AX, pChk1, p73, ANP, and β-MHC are shown. (B) Representative immunoblotting analysis of FNDC5 expression in the hearts of young (2-month-old) and aged (24-month-old) mice (n = 8). (C) AC-16 & H9C2 cells were treated with Doxorubicin (0.1 μM, 24 h) for 5 days. FNDC5 protein expression in non-senescent (passage numbers 5–7) and replicative-senescent (passage numbers 25–30) were determined by immunoblotting analysis (n = 5). (D) Scramble or lentiviral FNDC5-targeted shRNA was introduced into the hearts of group of young (2 months) or aged (24 months) mice via intracardiac injection as described (n = 4). After shRNA introduction, hearts were collected for analysis. (E) Correlation between FNDC5 expression in heart and patient age in control (black) and chemotherapy-exposed patients (red). Representative immunoblots and quantification of γH2AX, ATR, and pChk1 are shown. β-Actin serves as a loading control for immunoblots. Data were analyzed by student's t-test, and Two-way ANOVA with Sidak's post-hoc test. *$P < 0.05$, **$P < 0.01$, ***$P < 0.001$, ****$P < 0.0001$. ns = not significant. Data are presented as mean ± SEM.

FNDC5/irisin in control of mitochondrial function and oxidative stress, which, nonetheless, represents a critical contributor to the cardioprotective impacts of FNDC5/irisin in the doxorubicin-exposed heart. Similarly, the ability of FNDC5 to modulate mitochondrial function is unlikely to involve control of mitochondrial translation as this specifically requires phosphorylation of Chk1 at S296 [49], a site not impacted by FNDC5.

FNDC5 is a transmembrane protein with most of the protein in the

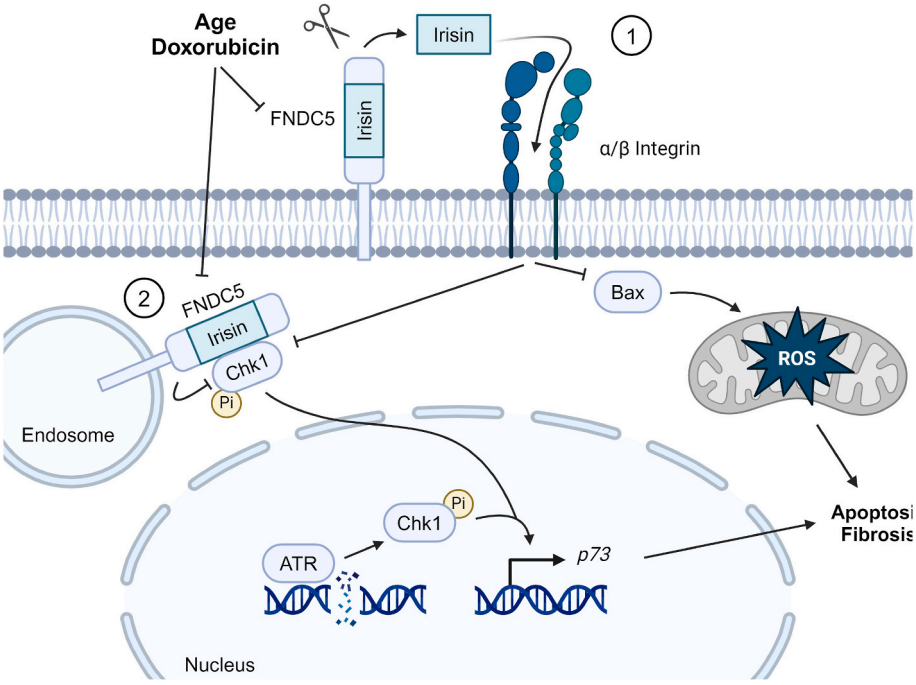

Fig. 9. – Schematic outlining the role of FNDC5 in Doxorubicin-induced cardiotoxicity. Our data support a model wherein FNDC5/irisin prevent Doxorubicin-dependent cardiomyocyte death by limiting ROS generation and activation of the mitochondrial apoptosis pathway and suppressing activation of the ATR/Chk1/p73 signaling axis. We have two hypotheses as to how FNDC5/irisin regulate Chk1: 1) Signaling via the irisin integrin receptor prevents Chk1 phosphorylation and activation or 2) FNDC5, possibly sequestered in the endocytic compartment, binds directly to Chk1 to block Chk1 phosphorylation. Image generated with biorender .com.

extracellular space including the fibronectin III domain containing the irisin sequence [61]. Chk1, conversely, shuttles between the cytoplasm and nucleus [62]. Thus, it is somewhat puzzling that these two proteins form a co-precipitable complex in cardiac myocytes. Whereas it is possible the Chk1-FNDC5 interaction is an artifact generated following disruption of cellular membranes, our *in silico* molecular modeling does predict stable complex formation between the two proteins. Thus, functional FNDC5 may, as is the case for other integrin family members such as fibronectin, direct intracellular signaling when internalized into an endocytic compartment [63]. Whereas modulation of FNDC5 expression fails to impact levels of Chk1 in the cytosol vs nucleus, FNDC5 does potently block nuclear accumulation of active, phosphorylated Chk1 (S345). These data rule out a function for FNDC5 in sequestration of Chk1 in the cytosol and indicated, instead, actions that require recruitment of an intermediary. As deletion of the fibronectin type III domain, which contains the irisin sequence, impairs FNDC5-Chk1 co-precipitation, it is also possible that irisin is produced intracellularly and capable of directing cell signaling independent of membrane receptors. However, our observations that cilengitide, an inhibitor of the irisin integrin receptor [48], prevents FNDC5 from suppressing Chk1 phosphorylation and irisin supplementation counteracts Chk1 activation following FNDC5 knockdown suggest that extracellular secretion of irisin contributes to FNDC5-dependent Chk1 regulation, at least in cultured cardiomyocytes.

Prior studies investigating the cardioprotective impacts of FNDC5/irisin were conducted utilizing a single large bolus dose of Dox (15 mg/kg, 8 days) or a shorter, low dose chronic treatment (4 mg/kg weekly for 4 weeks) [29] compared to our protocol (9 mg/kg, every other week for 10 weeks) [28] designed to better mimic chemotherapy treatment in human cancer patients. Thus, there may be multiple temporal phases wherein maintenance of FNDC5 expression may counteract the cardiotoxic impact of doxorubicin. Initially, the ability of FNDC5/irisin to suppress oxidative stress [28,29] is likely essential to preventing myocyte loss. However, given cardiac Chk1 has been linked to cardiac renewal and repair [64,65], targeting this pathway may aid in restoration of myocyte functional integrity. Chk1 might also represent a key target of FNDC5 during cardiogenesis, wherein FNDC5 has been previously linked to myocyte maturation and attenuation of cardiac senescence [30–33]. It is also important to note that, whereas FNDC5 depletion is clearly deleterious to cardiac function, we also found that FNDC5 overexpression in AC-16 cells, VCM or VCF led to up-regulation of heart failure markers ANP, Troponin T, and β-MHC indicating that excess FNDC5 expression may also be cardiotoxic. Indeed, another group also found that the enhancement in mitochondrial respiration in cardiomyocytes exposed to high levels of irisin increased oxidative stress and myocytes apoptosis [66], a result supported by our observation that FNDC5 overexpression in heart leads to induction of several key components of the mitochondrial electron transport chain. Similarly, treatment with Chk1 inhibitors or Chk1 genetic knockout results in cardiac atrophy and functional impairment due to loss of Chk1-dependent regulation of mitochondrial redox homeostasis [67]. As inhibition of Chk1 fails to prevent ROS generation following FNDC5 knockdown, we suspect that FNDC5/irisin may only regulate non-mitochondrial Chk1 or play a role in localizing Chk1 away from the mitochondria. Regardless, the therapeutic benefit of FNDC5 overexpression or irisin treatment in mice exposed to doxorubicin is likely derived, therefore, from counterbalancing doxorubicin driven FNDC5 depletion as opposed to the introduction of supraphysiological irisin levels.

We are not the first to observe that FNDC5 expression decreases with age in mice. However, whereas FNDC5 overexpression in heart prevented age-related impairments in cardiac function [33], we noted that the ability of FNDC5 to suppress doxorubicin-dependent γH2AX, p73, and ANP expression was lost in aged mice. In addition, the deleterious impact of FNDC5 knockdown on ATR/Chk1 expression was dramatically enhanced in older mice consistent with the already depleted FNDC5 stores. Intriguingly, whereas FNDC5 decreased Chk1 phosphorylation in young control mice, the opposite trend was observed in aged mice. In humans, there is a significant reduction in plasma irisin but not FNDC5 mRNA in skeletal muscle in older adults consistent with impaired processing of FNDC5 [68]. Paradoxically, however, expression of the

metalloproteinase ADAM10, shown to cleave FNDC5 to form irisin in heart [20], is increased in cardiac tissue from aged mice [69]. In our human heart samples, we did note age-dependent decreased in FNDC5 expression in both control and chemotherapy-exposed individuals supporting this assertion that decreased FNDC5 expression, possibly due to post-transcriptional regulation, may be the primary driving force for loss of local irisin production in the aged heart.

Irrespective of the exact cause, FNDC5 depletion with age may have severe consequences in the elderly particularly for cancer patients undergoing chemotherapy. Prior studies have demonstrated that, with age, antioxidant defense mechanisms and DNA repair processes become impaired [70–72] leading to accumulation of oxidative DNA damage [73,74], mitochondrial dysfunction, oxidative stress, and inflammation [75,76]. In addition, age is associated with exacerbation of chemotherapeutic-driven DNA damage [77] and myocyte death [78]. Thus, we hypothesize that FNDC5 functions to counterbalance age-dependent myocyte dysfunction and FNDC5 depletion may, in fact, contribute to the decline in resiliency to cytotoxic stress in the myocardium that occurs with age. However, as FNDC5 OE fails to improve heart failure indicators in aged mice exposed to doxorubicin, signaling downstream of FNDC5 clearly cannot fully counteract the deleterious impact of age in the presence of a potent myocyte poison. The enhanced ATR induction and γH2AX phosphorylation we observed in the absence of FNDC5 in older mice, then, likely reflects the myocytes' attempt to jump start DNA repair in the face of insurmountable DNA damage. Ultimately, this proves a futile endeavor given repair processes are impaired and inevitably leads to cell death.

Amongst the cell types present in heart, FNDC5 expression is highest in cardiomyocytes with some detectable expression in fibroblasts but negligible expression in endothelial cells or immune cell types [79]. As a caveat to our *in vivo* experiments, we should note that our viral delivery strategy does not confine FNDC5 overexpression to only myocytes and could result in aberrant ectopic FNDC5 expression in cell types that do not normally produce FNDC5 and/or release irisin. The addition of paracrine signaling between cardiomyocytes and neighboring cell types may explain, for example, why the impact of FNDC5 overexpression *in vivo* in heart on doxorubicin-dependent ATR/Chk1/p73 expression is more robust compared to the effects observed in cultured myocytes. Mimicking age- or doxorubicin-dependent FNDC5 depletion via introduction of FNDC5 shRNA into the heart may, however, more reliably identify functions of endogenous FNDC5. Indeed, FNDC5 knockdown in either myocytes or the murine myocardium led to oxidative stress, Chk1 phosphorylation, and induction of both p73 and Bax underscoring the likely contribution of myocyte intrinsic FNDC5 action and/or autocrine irisin signaling to doxorubicin-dependent cardiotoxicity. It is important to note that FNDC5 overexpression also decreased Chk1 phosphorylation in VCF. Though this could be due to direct binding between FNDC5 and Chk1 intracellularly, it may also reflect signaling via irisin and suggest that VCF express receptors for irisin and could be irisin responsive *in vivo*. The generation of cell type specific FNDC5 knockouts will be required to tease apart the autocrine, paracrine, and endocrine contributions of irisin signaling vs intracellular FNDC5 activity in heart.

Irisin has been proposed as a potential therapy for a host of human diseases including cardiovascular [80,81], neurological [82,83], and metabolic disorders [84] and cancer [85]. Our results suggest that obtaining a means to counterbalance FNDC5 depletion in the hearts of patients exposed to anthracyclines such as doxorubicin during cancer treatment might significantly mitigate the detrimental impact of doxorubicin on heart function. However, based on our data, there are two caveats to this assertion. First, irisin activity must be carefully tuned so as not to reach supraphysiological levels at which stage irisin signaling may place mitochondrial respiration into overdrive resulting in enhanced oxidative stress and cell death. Second, the beneficial impact of irisin on cardiac health is likely to decline as a function of age, a phenomenon that may limit the clinical utility of FNDC5/irisin-targeted therapies as a cardioprotective strategy in cancer patients, the majority of whom are over the age of 60.

CRediT authorship contribution statement

Manish Kumar: Writing – original draft, Methodology, Investigation, Formal analysis, Data curation, Conceptualization. **Abhishek Singh Sengar:** Validation, Methodology, Investigation, Formal analysis. **Anushree Lye:** Data curation, Formal analysis, Methodology. **Pranesh Kumar:** Validation, Resources, Methodology, Investigation. **Sukhes Mukherjee:** Resources, Methodology, Investigation, Formal analysis. **Dinesh Kumar:** Writing – original draft, Visualization, Validation, Software, Methodology, Investigation, Data curation, Conceptualization. **Priyadip Das:** Conceptualization, Formal analysis. **Suvro Chatterjee:** Resources, Investigation, Formal analysis. **Adele Stewart:** Writing – review & editing, Writing – original draft, Supervision, Software, Formal analysis, Conceptualization. **Biswanath Maity:** Writing – review & editing, Writing – original draft, Visualization, Supervision, Resources, Project administration, Methodology, Investigation, Funding acquisition, Formal analysis, Conceptualization.

Funding

This work was supported by Indian Council of Medical Research (ICMR – EMDR/SG/14/2023-0061) to BM.

Declaration of competing interest

This is to certify that no authors have conflict of interest in submitting the work for publication.

Acknowledgements

Mr. Manish Kumar thanks CSIR for the PhD research support and AcSIR for the registration. Dr. Pranesh Kumar who assisted in the mice experiments was in Aryakul College of Pharmacy & Research, Lucknow and has moved to the Institute of Pharmaceutical Sciences, University of Lucknow, India. We extend our gratitude to AIIMS Bhopal for authorizing mice experimental procedures. We also thank DR. Sayan Biswas, MD, Forensic Medicine, College of Medicine and Sagore Dutta Hospital, B.T. Road, Kamarhati, Kolkata, West Bengal for providing human samples.

Appendix A. Supplementary data

Supplementary data to this article can be found online at https://doi.org/10.1016/j.redox.2025.103527.

Data availability

No data was used for the research described in the article.

References

[1] M. Lotrionte, et al., Review and meta-analysis of incidence and clinical predictors of anthracycline cardiotoxicity, Am. J. Cardiol. 112 (2013) 1980–1984.
[2] M.A. Grenier, S.E. Lipshultz, Epidemiology of anthracycline cardiotoxicity in children and adults, Semin. Oncol. 25 (1998) 72–85.
[3] D.A. Mulrooney, et al., Cardiac outcomes in a cohort of adult survivors of childhood and adolescent cancer: retrospective analysis of the Childhood Cancer Survivor Study cohort, BMJ 339 (2009) b4606.
[4] S. Zhang, et al., Identification of the molecular basis of doxorubicin-induced cardiotoxicity, Nat. Med. 18 (2012) 1639–1642.
[5] K.J. Davies, J.H. Doroshow, Redox cycling of anthracyclines by cardiac mitochondria. I. Anthracycline radical formation by NADH dehydrogenase, J. Biol. Chem. 261 (1986) 3060–3067.
[6] J.H. Doroshow, K.J. Davies, Redox cycling of anthracyclines by cardiac mitochondria. II. Formation of superoxide anion, hydrogen peroxide, and hydroxyl radical, J. Biol. Chem. 261 (1986) 3068–3074.
[7] S. Kotamraju, C.R. Chitambar, S.V. Kalivendi, J. Joseph, B. Kalyanaraman, Transferrin receptor-dependent iron uptake is responsible for doxorubicin-

mediated apoptosis in endothelial cells: role of oxidant-induced iron signaling in apoptosis, J. Biol. Chem. 277 (2002) 17179–17187.
[8] G. Minotti, et al., Doxorubicin cardiotoxicity and the control of iron metabolism: quinone-dependent and independent mechanisms, Methods Enzymol. 378 (2004) 340–361.
[9] S. Deng, et al., Gp91phox-containing NAD(P)H oxidase increases superoxide formation by doxorubicin and NADPH, Free Radic. Biol. Med. 42 (2007) 466–473.
[10] Y. Zhao, et al., Nox2 NADPH oxidase promotes pathologic cardiac remodeling associated with Doxorubicin chemotherapy, Cancer Res. 70 (2010) 9287–9297.
[11] G. Minotti, P. Menna, E. Salvatorelli, G. Cairo, L. Gianni, Anthracyclines: molecular advances and pharmacologic developments in antitumor activity and cardiotoxicity, Pharmacol. Rev. 56 (2004) 185–229.
[12] C. Muller, et al., Cellular pharmacokinetics of doxorubicin in patients with chronic lymphocytic leukemia: comparison of bolus administration and continuous infusion, Cancer Chemother. Pharmacol. 32 (1993) 379–384.
[13] E. Lazzarini, et al., Stress-induced premature senescence is associated with a prolonged QT interval and recapitulates features of cardiac aging, Theranostics 12 (2022) 5237–5257.
[14] A.N. Linders, et al., Evaluation of senescence and its prevention in doxorubicin-induced cardiotoxicity using dynamic engineered heart tissues, JACC CardioOncol 5 (2023) 298–315.
[15] M. Demaria, et al., Cellular senescence promotes adverse effects of chemotherapy and cancer relapse, Cancer Discov. 7 (2017) 165–176.
[16] A.N. Linders, et al., A review of the pathophysiological mechanisms of doxorubicin-induced cardiotoxicity and aging, NPJ Aging 10 (2024) 9.
[17] Q. Liu, et al., Chk1 is an essential kinase that is regulated by Atr and required for the G(2)/M DNA damage checkpoint, Genes Dev. 14 (2000) 1448–1459.
[18] H. Zhao, H. Piwnica-Worms, ATR-mediated checkpoint pathways regulate phosphorylation and activation of human Chk1, Mol. Cell Biol. 21 (2001) 4129–4139.
[19] R. Zhao, et al., Nuclear ATR lysine-tyrosylation protects against heart failure by activating DNA damage response, Cell Rep. 42 (2023) 112400.
[20] Q. Yu, et al., FNDC5/Irisin inhibits pathological cardiac hypertrophy, Clin. Sci. (Lond.) 133 (2019) 611–627.
[21] M.F. Young, S. Valaris, C.D. Wrann, A role for FNDC5/Irisin in the beneficial effects of exercise on the brain and in neurodegenerative diseases, Prog. Cardiovasc. Dis. 62 (2019) 172–178.
[22] A. Silvestrini, et al., Circulating irisin levels in heart failure with preserved or reduced ejection fraction: a pilot study, PLoS One 14 (2019) e0210320.
[23] N.A. Abd El-Mottaleb, H.M. Galal, K.M. El Maghraby, A.I. Gadallah, Serum irisin level in myocardial infarction patients with or without heart failure, Can. J. Physiol. Pharmacol. 97 (2019) 932–938.
[24] I.C. Hsieh, et al., Serum irisin levels are associated with adverse cardiovascular outcomes in patients with acute myocardial infarction, Int. J. Cardiol. 261 (2018) 12–17.
[25] R.L. Li, et al., Irisin alleviates pressure overload-induced cardiac hypertrophy by inducing protective autophagy via mTOR-independent activation of the AMPK-ULK1 pathway, J. Mol. Cell. Cardiol. 121 (2018) 242–255.
[26] R. Li, et al., Irisin ameliorates angiotensin II-induced cardiomyocyte apoptosis through autophagy, J. Cell. Physiol. 234 (2019) 17578–17588.
[27] Y.T. Zhao, et al., Irisin ameliorates hypoxia/reoxygenation-induced injury through modulation of histone deacetylase 4, PLoS One 11 (2016) e0166182.
[28] C. Zhuo, et al., Irisin protects against doxorubicin-induced cardiotoxicity by improving AMPK-Nrf2 dependent mitochondrial fusion and strengthening endogenous anti-oxidant defense mechanisms, Toxicology 494 (2023) 153597.
[29] X. Zhang, et al., FNDC5 alleviates oxidative stress and cardiomyocyte apoptosis in doxorubicin-induced cardiotoxicity via activating AKT, Cell Death Differ. 27 (2020) 540–555.
[30] F. Rabiee, et al., Induced expression of Fndc5 significantly increased cardiomyocyte differentiation rate of mouse embryonic stem cells, Gene 551 (2014) 127–137.
[31] S. Nazem, et al., Fndc5 knockdown induced suppression of mitochondrial integrity and significantly decreased cardiac differentiation of mouse embryonic stem cells, J. Cell. Biochem. 119 (2018) 4528–4539.
[32] F.G. Zadegan, et al., Cardiac differentiation of mouse embryonic stem cells is influenced by a PPAR gamma/PGC-1alpha-FNDC5 pathway during the stage of cardiac precursor cell formation, Eur. J. Cell Biol. 94 (2015) 257–266.
[33] C. Hu, et al., Fibronectin type III domain-containing 5 improves aging-related cardiac dysfunction in mice, Aging Cell 21 (2022) e13556.
[34] A.S. Sengar, et al., RGS6 drives cardiomyocyte death following nucleolar stress by suppressing Nucleolin/miRNA-21, J. Transl. Med. 22 (2024) 204.
[35] M. Basak, et al., A RGS7-CaMKII complex drives myocyte-intrinsic and myocyte-extrinsic mechanisms of chemotherapy-induced cardiotoxicity, Proc. Natl. Acad. Sci. U. S. A. 120 (2023) e2213537120.
[36] A. Pramanick, et al., G protein beta5-ATM complexes drive acetaminophen-induced hepatotoxicity, Redox Biol. 43 (2021) 101965.
[37] C.S. Long, C.J. Henrich, P.C. Simpson, A growth factor for cardiac myocytes is produced by cardiac nonmyocytes, Cell Regul. 2 (1991) 1081–1095.
[38] S. Chakraborti, et al., Atypical G protein beta 5 promotes cardiac oxidative stress, apoptosis, and fibrotic remodeling in response to multiple cancer chemotherapeutics, Cancer Res. 78 (2018) 528–541.
[39] B. Kalyanaraman, et al., Measuring reactive oxygen and nitrogen species with fluorescent probes: challenges and limitations, Free Radic. Biol. Med. 52 (2012) 1–6.
[40] B.G. Pierce, Y. Hourai, Z. Weng, Accelerating protein docking in ZDOCK using an advanced 3D convolution library, PLoS One 6 (2011) e24657.
[41] B.G. Pierce, et al., ZDOCK server: interactive docking prediction of protein-protein complexes and symmetric multimers, Bioinformatics 30 (2014) 1771–1773.
[42] E. Krieger, G. Vriend, New ways to boost molecular dynamics simulations, J. Comput. Chem. 36 (2015) 996–1007.
[43] R. Raj, et al., Exquisite binding interaction of 18 beta-Glycyrrhetinic acid with histone like DNA binding protein of Helicobacter pylori: a computational and experimental study, Int. J. Biol. Macromol. 161 (2020) 231–246.
[44] R. Raj, et al., Epigallocatechin gallate with potent anti-Helicobacter pylori activity binds efficiently to its histone-like DNA binding protein, ACS Omega 6 (2021) 3548–3570.
[45] C.J. Dickson, et al., Lipid 14: the amber lipid force field, J. Chem. Theor. Comput. 10 (2014) 865–879.
[46] V. Hornak, et al., Comparison of multiple Amber force fields and development of improved protein backbone parameters, Proteins 65 (2006) 712–725.
[47] S.S. Negi, C.H. Schein, N. Oezguen, T.D. Power, W. Braun, InterProSurf: a web server for predicting interacting sites on protein surfaces, Bioinformatics 23 (2007) 3397–3399.
[48] H. Kim, et al., Irisin mediates effects on bone and fat via alphaV integrin receptors, Cell 175 (2018) 1756–1768.
[49] J. Zhang, et al., Systematic identification of anticancer drug targets reveals a nucleus-to-mitochondria ROS-sensing pathway, Cell 186 (2023) 2361–2379.
[50] J. Willis, Y. Patel, B.L. Lentz, S. Yan, APE2 is required for ATR-Chk1 checkpoint activation in response to oxidative stress, Proc. Natl. Acad. Sci. U. S. A. 110 (2013) 10592–10597.
[51] F.S. Korte, T.J. Herron, M.J. Rovetto, K.S. McDonald, Power output is linearly related to MyHC content in rat skinned myocytes and isolated working hearts, Am. J. Physiol. Heart Circ. Physiol. 289 (2005) H801–H812.
[52] J.C. Tardiff, et al., Expression of the beta (slow)-isoform of MHC in the adult mouse heart causes dominant-negative functional effects, Am. J. Physiol. Heart Circ. Physiol. 278 (2000) H412–H419.
[53] K. Das, et al., RGS11-CaMKII complex mediated redox control attenuates chemotherapy-induced cardiac fibrosis, Redox Biol. 57 (2022) 102487.
[54] S. Dewilde, K. Carroll, E. Nivelle, J. Sawyer, Evaluation of the cost-effectiveness of dexrazoxane for the prevention of anthracycline-related cardiotoxicity in children with sarcoma and haematologic malignancies: a European perspective, Cost Eff. Resour. Allocation 18 (2020) 7.
[55] P. Reichardt, M.D. Tabone, J. Mora, B. Morland, R.L. Jones, Risk-benefit of dexrazoxane for preventing anthracycline-related cardiotoxicity: re-evaluating the European labeling, Future Oncol. 14 (2018) 2663–2676.
[56] S. Deng, et al., The catalytic topoisomerase II inhibitor dexrazoxane induces DNA breaks, ATF3 and the DNA damage response in cancer cells, Br. J. Pharmacol. 172 (2015) 2246–2257.
[57] M.P. Cole, et al., The protective roles of nitric oxide and superoxide dismutase in adriamycin-induced cardiotoxicity, Cardiovasc. Res. 69 (2006) 186–197.
[58] D. Zhu, et al., Irisin improves endothelial function in type 2 diabetes through reducing oxidative/nitrative stresses, J. Mol. Cell. Cardiol. 87 (2015) 138–147.
[59] J. Peng, et al., Irisin protects against neuronal injury induced by oxygen-glucose deprivation in part depends on the inhibition of ROS-NLRP3 inflammatory signaling pathway, Mol. Immunol. 91 (2017) 185–194.
[60] J.A. Pan, et al., Irisin ameliorates doxorubicin-induced cardiac perivascular fibrosis through inhibiting endothelial-to-mesenchymal transition by regulating ROS accumulation and autophagy disorder in endothelial cells, Redox Biol. 46 (2021) 102120.
[61] S. Aydin, Three new players in energy regulation: preptin, adropin and irisin, Peptides 56 (2014) 94–110.
[62] Y. Katsuragi, N. Sagata, Regulation of Chk1 kinase by autoinhibition and ATR-mediated phosphorylation, Mol. Biol. Cell 15 (2004) 1680–1689.
[63] G. Mana, D. Valdembri, G. Serini, Conformationally active integrin endocytosis and traffic: why, where, when and how? Biochem. Soc. Trans. 48 (2020) 83–93.
[64] T.W. Wei, et al., Checkpoint kinase 1 stimulates endogenous cardiomyocyte renewal and cardiac repair by binding to pyruvate kinase isoform M2 C-domain and activating cardiac metabolic reprogramming in a porcine model of myocardial ischemia/reperfusion injury, J. Am. Heart Assoc. 13 (2024) e034805.
[65] Y. Fan, et al., Phosphoproteomic analysis of neonatal regenerative myocardium revealed important roles of checkpoint kinase 1 via activating mammalian target of rapamycin C1/ribosomal protein S6 kinase b-1 pathway, Circulation 141 (2020) 1554–1569.
[66] M.Y. Ho, et al., Excessive irisin increases oxidative stress and apoptosis in murine heart, Biochem. Biophys. Res. Commun. 503 (2018) 2493–2498.
[67] J.W. Chen, et al., SIRT3-dependent mitochondrial redox homeostasis mitigates CHK1 inhibition combined with gemcitabine treatment induced cardiotoxicity in hiPSC-CMs and mice, Arch. Toxicol. 97 (2023) 3209–3226.
[68] J.Y. Huh, et al., FNDC5 and irisin in humans: I. Predictors of circulating concentrations in serum and plasma and II. mRNA expression and circulating concentrations in response to weight loss and exercise, Metabolism 61 (2012) 1725–1738.
[69] D. Couchie, et al., Human plasma thioredoxin-80 increases with age and in ApoE (-/-) mice induces inflammation, angiogenesis, and atherosclerosis, Circulation 136 (2017) 464–475.
[70] B. Szczesny, A.W. Tann, S. Mitra, Age- and tissue-specific changes in mitochondrial and nuclear DNA base excision repair activity in mice: susceptibility of skeletal muscles to oxidative injury, Mech. Ageing Dev. 131 (2010) 330–337.
[71] P. Wenzel, et al., Manganese superoxide dismutase and aldehyde dehydrogenase deficiency increase mitochondrial oxidative stress and aggravate age-dependent vascular dysfunction, Cardiovasc. Res. 80 (2008) 280–289.

[72] A. Vaidya, et al., Knock-in reporter mice demonstrate that DNA repair by non-homologous end joining declines with age, PLoS Genet. 10 (2014) e1004511.
[73] M.L. Hamilton, et al., Does oxidative damage to DNA increase with age? Proc. Natl. Acad. Sci. U. S. A. 98 (2001) 10469–10474.
[74] A. Herrero, G. Barja, Effect of aging on mitochondrial and nuclear DNA oxidative damage in the heart and brain throughout the life-span of the rat, J Am Aging Assoc 24 (2001) 45–50.
[75] D. Yeo, C. Kang, L.L. Ji, Aging alters acetylation status in skeletal and cardiac muscles, Geroscience 42 (2020) 963–976.
[76] C. Canugovi, et al., Increased mitochondrial NADPH oxidase 4 (NOX4) expression in aging is a causative factor in aortic stiffening, Redox Biol. 26 (2019) 101288.
[77] H. Niedermuller, Age dependency of DNA repair in rats after DNA damage by carcinogens, Mech. Ageing Dev. 19 (1982) 259–271.
[78] R. Chen, G. Zhang, K. Sun, A.F. Chen, Aging-associated ALKBH5-m(6)A modification exacerbates doxorubicin-induced cardiomyocyte apoptosis via AT-rich interaction domain 2, J. Am. Heart Assoc. 13 (2024) e031353.
[79] E. Sjostedt, et al., An atlas of the protein-coding genes in the human, pig, and mouse brain, Science 367 (2020).
[80] Y. Liu, et al., The cerebroprotection and prospects of FNDC5/irisin in stroke, Neuropharmacology 253 (2024) 109986.
[81] T. Zhang, Q. Yi, W. Huang, J. Feng, H. Liu, New insights into the roles of Irisin in diabetic cardiomyopathy and vascular diseases, Biomed. Pharmacother. 175 (2024) 116631.
[82] E. Kim, R.E. Tanzi, S.H. Choi, Therapeutic potential of exercise-hormone irisin in Alzheimer's disease, Neural Regen Res 20 (6) (2025) 1555–1564.
[83] M. Yang, et al., Myokines: novel therapeutic targets for diabetic nephropathy, Front. Endocrinol. 13 (2022) 1014581.
[84] J.F. Bao, Q.Y. She, P.P. Hu, N. Jia, A. Li, Irisin, a fascinating field in our times, Trends Endocrinol. Metabol. 33 (2022) 601–613.
[85] M. Pinkas, T. Brzozowski, The role of the myokine irisin in the protection and carcinogenesis of the gastrointestinal tract, Antioxidants 13 (2024).